A gammaherpesvirus-secreted activator of Vβ4+ CD8+ T cells regulates chronic infection and immunopathology

Andrew G. Evans,[1,2] Janice M. Moser,[1,2] Laurie T. Krug,[1,2] Veranika Pozharskaya,[3] Ana L. Mora,[4] and Samuel H. Speck[1,2]

[1]Emory Vaccine Center, [2]Department of Microbiology and Immunology, [3]Department of Pediatrics, and [4]Department of Medicine, Emory University School of Medicine, Atlanta, GA 30322

Little is known about herpesvirus modulation of T cell activation in latently infected individuals or the implications of such for chronic immune disorders. Murine gammaherpesvirus 68 (MHV68) elicits persistent activation of CD8+ T cells bearing a Vβ4+ T cell receptor (TCR) by a completely unknown mechanism. We show that a novel MHV68 protein encoded by the M1 gene is responsible for Vβ4+ CD8+ T cell stimulation in a manner reminiscent of a viral superantigen. During infection, M1 expression induces a Vβ4+ effector T cell response that resists functional exhaustion and appears to suppress virus reactivation from peritoneal cells by means of long-term interferon-γ (IFNγ) production. Mice lacking an IFNγ receptor (IFNγR$^{-/-}$) fail to control MHV68 replication, and Vβ4+ and CD8+ T cell activation by M1 instead contributes to severe inflammation and multiorgan fibrotic disease. Thus, M1 manipulates the host CD8+ T cell response in a manner that facilitates latent infection in an immunocompetent setting, but promotes disease during a dysregulated immune response. Identification of a viral pathogenecity determinant with superantigen-like activity for CD8+ T cells broadens the known repertoire of viral immunomodulatory molecules, and its function illustrates the delicate balance achieved between persistent viruses and the host immune response.

CORRESPONDENCE
Samuel H. Speck:
sspeck@emory.edu

Abbreviations used: BAC, bacterial artificial chromosome; ICC, intracellular cytokine; IM, infectious mononucleosis; MEF, mouse embryonic fibroblast; ORF, open reading frame; PEC, peritoneal exudate cell; SAP, SLAM-associated protein.

Herpesvirus pathogenesis is closely linked to host immune status. The majority of herpesvirus-infected individuals never experience clinical symptoms, but infection among the immunocompromised is a risk factor for numerous complications (1). MHV68 is a γ2 herpesvirus, closely related to the human pathogens EBV and Kaposi's sarcoma–associated herpesvirus (2, 3). Like human herpesviruses, the vast majority of MHV68-infected immunocompetent mice do not develop disease; however, chronic infection of IFNγR$^{-/-}$ mice is a notable exception (4–6). IFNγ directly inhibits viral replication and/or reactivation from latency in specific cell types, i.e., macrophages but not B cells (7, 8). In the absence of an IFNγ response in vivo, persistent MHV68 replication emerges several weeks after infection and promotes a lethal inflammatory disorder consisting of lymphocytic infiltrates in multiple organs and fibrotic changes in the spleen, lymph nodes, and lung (6, 9). The resulting pulmonary disease is studied as a model for human idiopathic pulmonary fibrosis (IPF) associated with gammaherpesvirus infection (10–12), and persistent virus replication in the great elastic arteries gives rise to lesions that bear resemblance to clinical vasculitides such as Takayasu's arteritis and Kawasaki disease (13–15). Although the precise etiology of organ fibrosis is unknown, and probably wide ranging in both humans and animals models, three distinct elements are essential in the pathogenesis of MHV68-induced fibrotic disease: (a) persistent viral replication; (b) host T cells; and (c) a unique viral gene of unknown function, designated M1 (6, 11, 15, 16).

The M1 gene of MHV68 suppresses reactivation from latency in immunocompetent C57BL/6 mice, but the mechanism by which it exerts this effect, and the extent of immune system involvement, is unknown (16). The M1 gene is unique to MHV68 and is encoded within a locus of multiple unique open reading frames (ORFs).

J.M. Moser's present address is VaxDesign Corporation, Orlando, FL 32826.

The online version of this article contains supplemental material.

The Journal of Experimental Medicine

Each ORF is dispensable for in vitro growth, but critical for regulating aspects of in vivo infection (16–23). Based on the capacity of M1 to inhibit reactivation in vivo, it was unexpected that M1 also promotes fibrotic disease in IFNγR$^{-/-}$ mice—a T cell–mediated process that was previously thought to result directly from persistent virus replication (11, 16).

Antiviral CD8$^+$ T cell responses help control both lytic and latent MHV68 infection (24–28). Eventually, antigen-specific T cell responses become down-regulated, exhibit little evidence of continued activation, and contract in the manner typical of memory T cell responses. (29–31). A notable exception to this pattern is the Vβ4$^+$ CD8$^+$ T cell response. In the third week after infection, cells bearing a Vβ4$^+$ TCR rapidly proliferate, rise to the level of 30–60% of peripheral CD8$^+$ T cells in C57BL/6 mice, and remain at elevated levels throughout the course of latency (32, 33). The Vβ4$^+$ CD8$^+$ T cell response has been proposed as a mouse model for EBV-induced infectious mononucleosis (IM), but the degree of similarity between the two phenomena is ill-defined (34, 35). A latency-specific stimulus for the Vβ4$^+$ response is suggested because latency-deficient MHV68 mutants fail to generate a response during lytic infection and because B cells (the major latency reservoir for MHV68) are required for Vβ4$^+$ CD8$^+$ T cell expansion (30, 36–38). This response is not limited to C57BL/6 mice, but occurs to varying degrees in a wide variety of inbred mice, demonstrating preferential expansion among strains expressing the H2^b MHC haplotype (32, 39). Superantigen-driven proliferation was proposed for this response because it is confined to cells expressing a single variable region in the TCR β chain and it is not definitively MHC restricted (32). However, Vβ4$^+$ CD8$^+$ T cell expansion is not broadly polyclonal (based on complementarity-determining region–3 size analysis and V-D-J junctional region diversity) as demonstrated for classical CD4$^+$ superantigen responses (40). Numerous lines of evidence have shown that Vβ4$^+$ CD8$^+$ T cell activation does not require classical MHC class Ia antigen presentation, including studies of mice deficient for MHC class Ia molecules (H-2K$^{b-/-}$ × H-2D$^{b-/-}$), β2 microglobulin (β2m$^{-/-}$), and the transporter associated with antigen processing (TAP$^{-/-}$) (37, 41). These data either implicate a role for β2m-independent, nonpolymorphic MHC class Ib molecules or an unconventional, MHC-independent mechanism of CD8$^+$ T cell activation. Ultimately, the identity of the Vβ4$^+$ CD8$^+$ T cell stimulatory ligand and its biological significance has remained elusive.

The goal of this study was to investigate a potential immunomodulatory function for the MHV68 M1 gene product that could explain its role in regulating virus reactivation and disease. This first led to the surprising finding that the M1-dependent immunopathology observed in MHV68-infected IFNγR$^{-/-}$ mice is associated with activation of the enigmatic Vβ4$^+$ CD8$^+$ T cell population and second to the discovery that the M1 antigen of MHV68 is capable of stimulating Vβ4$^+$ CD8$^+$ T cells both in vivo and in vitro in a manner consistent with superantigen-like behavior. These data are potentially ground-breaking because they identify a secreted viral protein that stimulates murine CD8$^+$ T cells in an apparently novel fashion and demonstrate that such activity either contributes to immunological control of infection or virus-induced disease, depending on the status of the host's immune system.

RESULTS

MHV68 immunopathology induced by the M1 ORF is associated with the presence of Vβ4$^+$ CD8$^+$ T cells

We previously demonstrated that IFNγR$^{-/-}$ mice infected with an M1-deficient virus do not exhibit the mortality or fibrotic changes associated with WT MHV68 infection (16). It was independently shown that both CD8$^+$ and CD4$^+$ T cells were required for splenic fibrosis during MHV68 infection (6). Therefore, we compared the T cell response elicited by WT and M1 mutant MHV68 infection in IFNγR$^{-/-}$ mice. We extended the initial observation (which used a mutant containing a large insertion into the M1 ORF) using a mutant virus with a targeted 511-bp deletion (M1Δ511) spanning the 5′ end of M1 ORF (16). In agreement with previously published data (16), the spleens of M1Δ511-infected mice exhibited a normal histological appearance as compared with M1 marker rescue (M1.MR) control virus, which promoted extensive fibrotic scarring and decreased cellularity in infected spleens by 1 mo after infection (Fig. 1 A). Beyond the spleen, M1.MR virus induced extensive lymphocytic infiltrates throughout the lung and liver, whereas M1Δ511 virus did not produce any signs of disease (Fig. 1 A).

When the T cell response for each group of mice was examined at the same time point, the absence of inflammatory changes in M1Δ511-infected animals correlated with the absence of an activated CD8$^+$ T cell population (CD11a^{hi}, CD44$^+$, and CD62L^{lo}; unpublished data). Surprisingly, the lack of activated T cells in M1Δ511-infected mice could be attributed to a total deficiency of Vβ4$^+$ CD8$^+$ T cell expansion (Fig. 1 B). A direct association between Vβ4$^+$ CD8$^+$ T cell activation and disease was suggested by immunohistochemical staining of the pulmonary infiltrates from M1.MR-infected mice, demonstrating that the inflammatory lesions contained substantial numbers of Vβ4$^+$ and CD8$^+$ T cells (Fig. 1 C). Importantly, the titer of persistently replicating virus in the diseased organs of M1.MR-infected mice was comparable to the titer in the healthy tissues from M1Δ511-infected mice (Fig. 1 D). In agreement with the absence of pulmonary inflammation at 28 d after infection, long-term fibrotic changes were not detected in the lungs of M1Δ511-infected mice as late as 180 d after infection as compared with those infected with WT MHV68 (Fig. 1 E). Thus, the failure of M1Δ511 to induce chronic T cell–mediated fibrosis correlated with the absence of Vβ4$^+$ CD8$^+$ T cell activation and corresponding inflammation, strongly suggesting that these T cells play a critical role in the pathogenesis of fibrotic disease in IFNγR$^{-/-}$ mice. These data also demonstrate that persistent virus replication is insufficient to cause fibrotic disease in the absence of M1 expression and the associated Vβ4$^+$ CD8$^+$ T cell response.

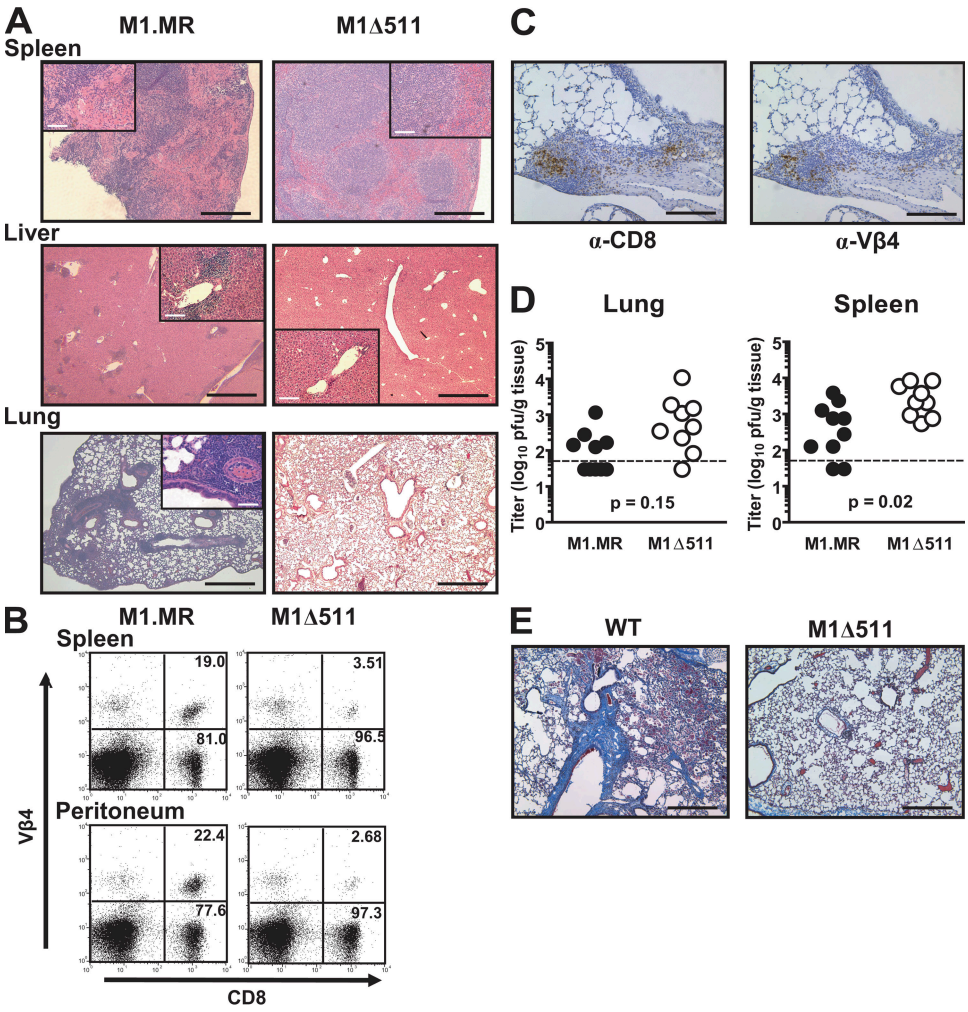

Figure 1. M1 and the Vβ4⁺ CD8 T cell response are required for virus-induced inflammation and fibrosis in IFNγ-unresponsive mice. IFNγR$^{-/-}$ mice were infected with 10^3 PFU of the indicated virus intranasally and analyzed at 28 d after infection in A–D. (A) Hematoxylin and eosin staining of pathological changes in the spleen, liver, and lung. Bars: (spleen and liver) black, 200 µm; (spleen and liver) white, 80 µm; (lung) black, 400 µm; (lung) white, 40 µm. (B) Representative flow cytometric plots of Vβ4⁺ CD8⁺ T cell populations from mice infected with each virus. Numeric values are given for the proportion of CD8⁺ cells (right quadrants only). (C) Immunohistochemical staining for CD8⁺ cells and Vβ4⁺ cells in inflammatory lesions of the lung from M1.MR-infected animals, as indicated by brown chromogen deposition. Bars, 160 µm. (D) Persistent replication of each virus from each organ as measured by plaque assay. (E) Masson trichrome staining of lung sections at 180 d after infection from mice infected with 10^5 PFU of WT or M1Δ511 virus. Blue indicates areas of collagen deposition. Bars, 200 µm.

The M1 ORF is required for Vβ4⁺ CD8⁺ T cell expansion

The Vβ4⁺ CD8⁺ T cell response is a highly unusual example of an antiviral T cell response because of its activation profile, kinetics, and apparent MHC independence (32, 33, 37, 39, 41). The hypothesis that Vβ4⁺ CD8⁺ T cell activation is the result of a viral superantigen was proposed, but a candidate T cell ligand has never been identified (32). Having demonstrated that loss of M1 ablates this response, we considered that M1 might be the putative viral T cell stimulatory ligand. To focus on M1 and rule out other viral factors, we set about a more rigorous genetic mapping of adjacent mutations in the MHV68 genome that might affect Vβ4⁺ T cell activation. In addition to the aforementioned M1Δ511 mutant and control virus, a panel of individual viral mutants was compiled consisting of three recombinant viruses harboring translation stop codons within each of the M1 neighboring genes (M2, M3, and M4), as well as a large-scale deletion mutant (Δ9473) that spans nearly 9.5 kb and encompasses the entire left end of the genome, including M1 (Fig. 2 C) (17–19, 22). After infection of immunocompetent C57BL/6 mice with each virus, the extent of Vβ4⁺ CD8⁺ T cell expansion was assessed at the normal peak of this response at 28 d after infection. Only the M1Δ511 virus and the Δ9473 virus failed to induce Vβ4⁺ CD8⁺ T cell expansion, whereas the extent of Vβ4⁺ CD8⁺ T cell expansion was comparable among all other viral mutants tested (Fig. 2, A and B). Importantly, the M1Δ511 mutant both replicates and establishes latency in vivo at levels comparable to WT virus; thus, the failure of the M1 mutant virus

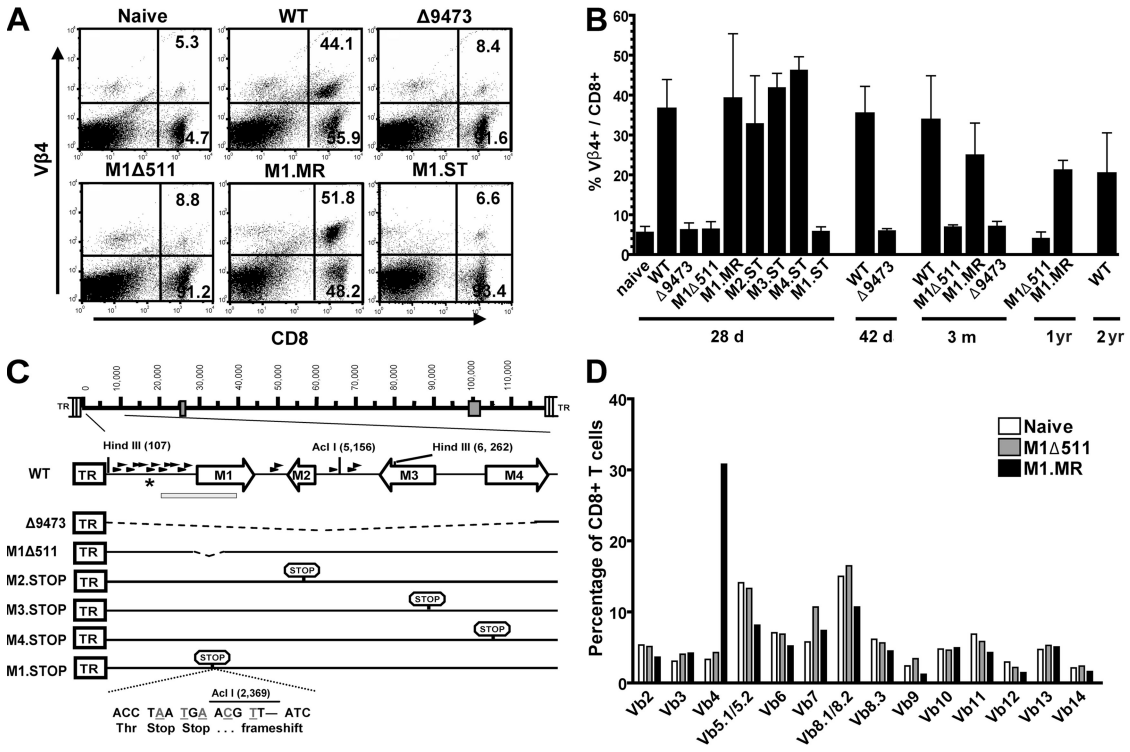

Figure 2. The M1 ORF is required for Vβ4⁺ CD8⁺ T cell expansion. (A) C57BL/6 mice were infected intranasally with 10^3 PFU of each viral genotype as indicated, and the Vβ4⁺ CD8⁺ splenocyte population was measured at 28 d after infection. Representative flow plots for five viral genotypes, as well as uninfected mice, are shown. Numeric values are given for the proportion of CD8⁺ cells (right hand quadrants) only. (B) Graphical representation of the Vβ4⁺ population size elicited by all viral genotypes, as described in part A, at the indicated times after infection. Data are pooled from 1–3 independent experiments with 3–5 mice per group. Error bars denote the SD. (C) Schematic diagram of the γHV68 genome highlighting the 9.5-kb region of interest with the genetic structure of mutants Δ9473 (16), M1Δ511 (15), M2.STOP (18), M3.STOP (22), and M4.STOP (17) shown in relation. The novel mutations that constitute the M1.STOP virus are underlined (five base pair substitutions yielding back-to-back translational stop codons, followed by a single deletion producing a downstream frameshift). Large and small triangles correspond to the eight viral tRNAs and nine viral microRNAs, respectively (44). (D) The Vβ repertoire of CD8⁺ splenocytes was examined 28 d after intranasal infection of a C57BL/6 mouse with 10^3 PFU of the indicated virus.

to induce Vβ4⁺ CD8⁺ T cell expansion was not caused by an attenuated viral infection, as has been shown with other latency-deficient mutants (21, 30). In addition, the absence of Vβ4⁺ CD8⁺ T cell expansion after M1Δ511 infection was not the result of delayed kinetics of T cell activation because both M1Δ511 and Δ9473 viruses did not exhibit any evidence of Vβ4⁺ T cell expansion at 42 d, 3 mo, and 1 yr after infection, whereas WT and M1.MR virus demonstrated the characteristic protracted response (Fig. 2 B). Finally, in the absence of a Vβ4⁺ CD8⁺ T cell response during M1Δ511 infection, no other Vβ subset was seen to expand in compensation (Fig. 2 D).

Because the region immediately adjacent to the M1 gene contains several viral tRNA-like and putative miRNA genes (42–44), it was possible that the 511-bp deletion spanning the 5′ end of the M1 gene might also impact expression of one or more of these genes (Fig. 1 C). Thus, to more definitively determine whether the Vβ4⁺ CD8⁺ T cell expansion and activation maps to the M1 ORF, we engineered a new MHV68 M1 mutant, M1.STOP, by altering 6 bp at the 5′ end of the M1 ORF to introduce two translation stop codons and a frameshift mutation (Fig. 2 C). Notably, infection of C57BL/6 mice with the M1.STOP mutant virus fully recapitulated the failure of previous M1-deficient viruses to induce Vβ4⁺ CD8⁺ T cell expansion during latency (Fig. 2, A and B). Likewise, M1.STOP infection failed to induce spleen, lung, or liver inflammatory lesions in infected IFNγR$^{-/-}$ mice, as shown for M1Δ511 virus in Fig. 1 (not depicted). Thus, we concluded that the MHV68 M1 gene product is critical in promoting the expansion and activation of the Vβ4⁺ CD8⁺ T cell population.

Control of virus reactivation is dependent on the M1 ORF and Vβ4⁺ CD8⁺ T cell expansion

Disruption of the M1 ORF results in enhanced reactivation from latency in peritoneal exudate cells (PECs) recovered from infected C57BL/6 mice, and thus the M1-encoded gene product was proposed to act as an inhibitor of virus reactivation (16). Indeed, both M1.STOP and M1Δ511 mutants exhibit roughly a 10-fold higher frequency of reactivation from PECs at 6 wk after infection as compared with M1.MR and WT MHV68, whereas the frequency of infected cells was the same for each (Fig. 3 B). We postulated that the capacity of M1 to suppress reactivation resulted from large-scale Vβ4⁺ T cell activation and their acquisition of antiviral effector functions.

Notably, neither M1-dependent reactivation nor Vβ4$^+$ CD8$^+$ T cell expansion was influenced by viral dose (Fig. S1, available at http://www.jem.org/cgi/content/full/jem.20071135/DC1). To assess whether the control of reactivation and the stimulation of CD8$^+$ T cells are functionally linked, reactivation of M1-null viruses was examined under conditions in which the Vβ4$^+$ CD8$^+$ T cell expansion and activation are not apparent. First, reactivation from latency was measured for each virus before the expansion of Vβ4$^+$ CD8$^+$ T cells. We confirmed that Vβ4$^+$ CD8$^+$ T cell expansion begins 18–20 d after infection and that the response does not vary by route of infection (unpublished data). Mice were examined at 16–18 d after intraperitoneal inoculation, and the frequencies of reactivating PECs did not significantly differ between M1.STOP, M1Δ511, M1.MR, or WT viruses (Fig. 3 A). Thus, M1-dependent control of reactivation can only be detected after the expansion of the Vβ4$^+$ CD8$^+$ T cell population. A model for control of reactivation by Vβ4$^+$ CD8$^+$ T cells implies that their persistent state of activation should predict long-term viral control that is dependent on M1. Accordingly, the frequency of PECs reactivating virus at 195–220 d after infection from M1Δ511-infected mice was >10-fold higher than observed with the M1.MR-infected mice, whereas the frequency of viral genome-positive cells was only slightly skewed in favor of the mutant (Fig. 3 C). This relatively small increase in viral load cannot account for the greatly elevated reactivation seen with M1Δ511. Thus, the kinetics of Vβ4$^+$ CD8$^+$ T cell expansion correlates well with the time course over which M1 represses reactivation from latently infected PECs.

To further investigate the association between M1 control of virus reactivation and activation of Vβ4$^+$ CD8$^+$ T cells, we took advantage of intrinsic genetic differences between inbred strains of mice. This approach was necessary because attempts to eliminate Vβ4$^+$ T cells via antibody depletion proved unsuccessful (see Discussion). The extent of MHV68-driven Vβ4$^+$ CD8$^+$ T cell expansion varies widely between mouse strains in accordance with their MHC haplotype. Specifically, mice bearing an H-2^b MHC haplotype (e.g., C57BL/6) show a greater Vβ4$^+$ CD8$^+$ T cell expansion than animals expressing H-2^d haplotypes (39). Thus, we reasoned that the lack of a robust Vβ4$^+$ CD8$^+$ T cell response in mice with an H-2^d haplotype would minimize the capacity of M1 to influence reactivation from latency. To test this hypothesis, BALB/c mice (H-2^d) were infected with M1.STOP and WT virus, and the impact of M1 on virus reactivation and Vβ4$^+$ CD8$^+$ T cell expansion was examined. WT MHV68 infection of BALB/c mice resulted in a modest, approximately twofold expansion of the Vβ4$^+$ CD8$^+$ T cell population in the first month after infection, which was no longer evident by 1 yr after infection (Fig. 4, A and B). Notably, this small expansion was also observed with M1.MR virus, but not upon infection with the M1Δ511 mutant (Fig. 4 A). Next, BALB/c mice were infected via intraperitoneal inoculation and PEC reactivation was examined at 6 wk after infection. As predicted, the frequency of reactivation from latently infected PECs did not differ significantly between M1.STOP and WT virus-infected mice (Fig. 4 C). Thus, we concluded that M1 is incapable of influencing virus reactivation in mice that are intrinsically unable to mount a robust

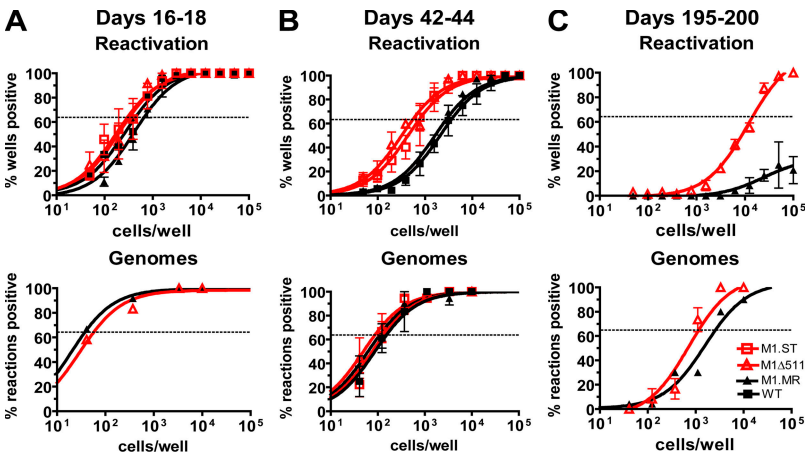

Figure 3. M1 function suppresses reactivation from latency in accordance with Vβ4$^+$ CD8$^+$ T cell activation. C57BL/6 mice were infected by intraperitoneal inoculation with 10^2 or 10^6 PFU of each indicated virus, and the extent of reactivation and latency among the PECs was quantified by limiting dilution analyses. Time points were chosen before, after, and long after the Vβ4$^+$ CD8$^+$ T cell expansion had occurred, at 16–18 (A), 42–44 (B), and 195–200 d (C) after infection, respectively. The frequency of reactivation was measured by plating live cells in a limiting dilution series onto a MEF indicator monolayer and scoring the frequency of wells positive for cytopathic effect (CPE; top). The relative contribution of preformed infectious virus was evaluated in parallel by mechanically disrupting the maximum number of cells and plating the cell lysates in parallel. In each of the experiments, the contribution of preformed virus accounted for ≤1% of the CPE produced by plating intact cells (not depicted). The frequency of latently infected, viral genome-positive cells was measured by subjecting a limiting dilution series of cells to lysis and proteinase K digestion, followed by highly sensitive nested PCR capable of detecting a single copy of the MHV68 genome (bottom). Graphs represent the combined data from three independent experiments with 4–5 animals per group. Error bars denote the SD.

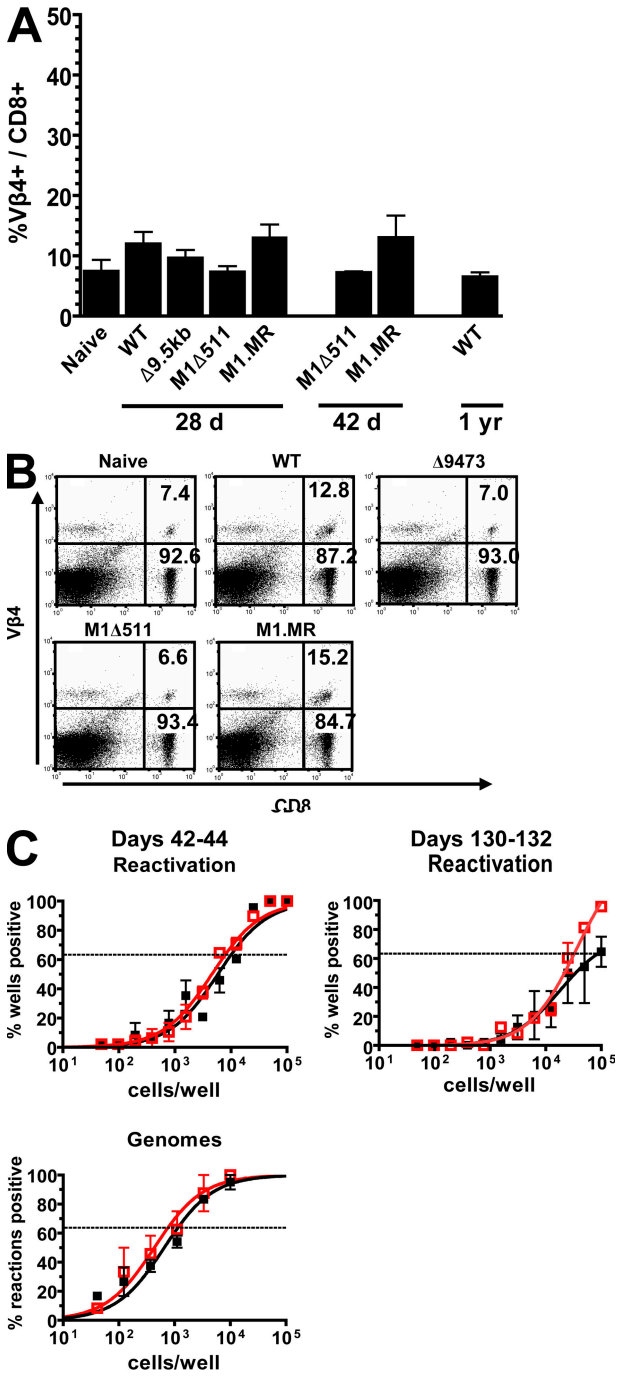

Figure 4. M1 is incapable of regulating virus reactivation in the absence of robust Vβ4⁺ CD8⁺ T cell expansion among BALB/c mice. (A) BALB/c mice were infected intranasally with 10^3 PFU of the indicated viruses, and the proportion of Vβ4⁺ CD8⁺ splenocytes was quantified at the indicated times. Data are pooled from 1–2 independent experiments with 2–4 mice per group. (B) Representative flow plots of the Vβ4⁺ CD8⁺ T cell expansion at 28 d after infection from mice in A. Numeric values are given for the proportion of CD8⁺ cells (right quadrants) only. (C) Reactivation from BALB/c PECs was measured by limiting dilution assay from mice infected via intraperitoneal inoculation with 10^6 PFU of the indicated viral genotype either 42–44 or 130–132 d earlier. The experimental conditions and assays performed here are identical to the experiments performed on C57BL/6 mice in Fig. 3 B, with the exception of late time point being performed at ~4 mo after infection. Red line and symbols, M1.Stop; black line and symbols, WT MHV68. Error bars denote the SD.

Vβ4⁺ CD8⁺ T cell response. Collectively, the data showing identical kinetics of Vβ4⁺ T cell expansion and M1-dependent reactivation in C57BL/6 mice and the absence of an M1-associated reactivation phenotype in mice that lack robust expansion of Vβ4⁺ CD8⁺ T cells, argue that the M1-dependent control of virus reactivation from latently infected PECs functions through an activated Vβ4⁺ CD8⁺ T cell mediator.

Vβ4⁺ CD8⁺ T cells exhibit an effector memory phenotype without signs of functional exhaustion

The capacity of Vβ4⁺ CD8⁺ T cells to regulate chronic viral reactivation implies that these cells are potent antiviral effector cells. At the peak of the Vβ4⁺ CD8⁺ T cell response within the spleen, these cells are CD11a (LFA-1)^{hi}, CD44⁺, CD62L (L-selection)^{lo}, and CD127 (IL-7Rα)^{lo} (Fig. 5 A), although negative for CD25 and CD69 expression as previously reported (not depicted) (33). Each feature is maintained as late as 6 mo after infection, with the exception of CD127, which was up-regulated by this time (Fig. 4 A and unpublished data), indicating that the persistence of the Vβ4⁺ CD8⁺ T cell response was analogous to the maintenance of an effector memory T cell population (45). The Vβ4⁺ population also expresses the C-type lectin inhibitory receptor NKG2A, which is often found on NK and activated CD8⁺ T cells (Fig. 5 A) (46). In contrast, Vβ4⁺ CD8⁺ T cells did not express the PD-1 inhibitory receptor at any time between 28 d to 6 mo after infection, as is characteristic of activated and/or chronically exhausted CD8⁺ T cells (Fig. 5 A and not depicted) (47).

Ongoing proliferation among the expanded Vβ4⁺ CD8⁺ T cell population appears to be on par with the rate of homeostatic proliferation among all other CD8⁺ T cells in infected mice, as determined by in vivo BrdU incorporation over a 1-wk course of treatment during the fourth month after infection (Fig. 5 A). Cytokine production was measured as an indicator of T cell function by ex vivo stimulation with anti-CD3, and revealed potent production of both IFNγ and TNF-α by Vβ4⁺ CD8⁺ T cells from 28 d to 6 mo after infection (Figs. 5, A and B, and Fig. 6, C–E). Notably, in the absence of M1 expression and Vβ4⁺ CD8⁺ T cell expansion, the proportion of CD8⁺ T cells capable of eliciting IFNγ upon ex vivo stimulation was drastically reduced (Fig. 5 B and Fig. S2, available at http://www.jem.org/cgi/content/full/jem.20071135/DC1). Thus, the Vβ4⁺ CD8⁺ T cell response that resists functional exhaustion likely represents a key source of IFNγ production for the regulation of viral reactivation.

M1 encodes a secreted protein capable of stimulating Vβ4⁺ CD8⁺ T cells specifically

To assess the possibility that the M1 gene product directly stimulates CD8⁺ T cells in a manner analogous to a superantigen,

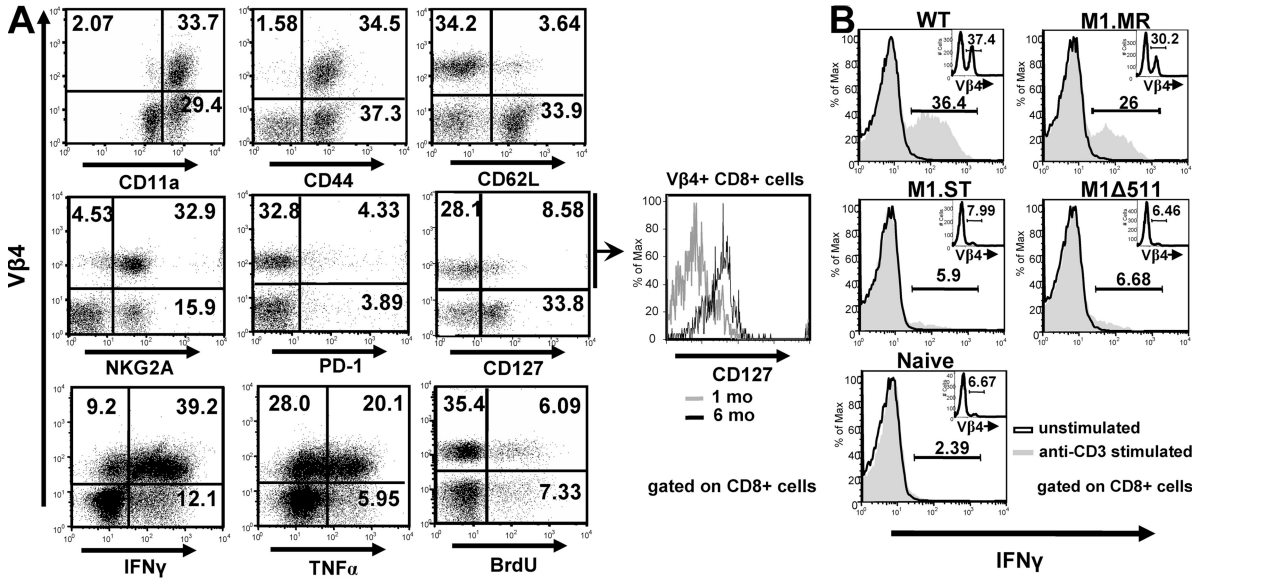

Figure 5. Vβ4⁺ CD8⁺ cells exhibit effector memory T cell characteristics, including potent IFNγ production during γHV68 latency. (A) CD8⁺ T cells were examined for multiple markers of T cell activation, proliferation, and effector function after intranasal infection of C57BL/6 mice with 10^3 PFU of WT MHV68. All plots are gated on total CD8⁺ splenocytes and are representative of multiple samples from independent experiments measured at 28 d after infection. Identical analyses were performed as late as 6 mo after infection, and the only significant change observed was the up-regulation of CD127 as shown in the offset panel (gray histogram, 1 mo after infection; black histogram, 6 mo after infection). Representative plots for ICC staining are shown from 2.5 mo after infection, at which time splenocytes were cultured in the presence of Brefeldin A and 1 μg/ml of soluble anti-CD3 monoclonal antibody to elicit cytokine production. BrdU incorporation was measured at 4 mo after infection after a 1-wk course of BrdU administration in the drinking water (0.8 mg/ml) of infected mice. Numeric values are given for the proportion of total CD8⁺ cells in each quadrant. (B) ICC staining for IFNγ production was performed as in A on CD8⁺ splenocytes from C57BL/6 mice at 28 d after infection with each indicated viral genotype. Insets show frequency of Vβ4⁺ cells from unstimulated controls for each sample. Plots are representative of results for 2–3 animals per condition.

as originally speculated for the Vβ4⁺ stimulatory ligand (32), we generated recombinant protein and tested its capacity to activate primary T cells. The putative M1 antigen is predicted to be a 47-kD secreted protein, based on the presence of a 19-aa, N-terminal consensus secretory signal peptide. Notably, both the neighboring M3 and M4 genes of MHV68 encode secreted proteins, and the low level homology shared between M1, M3, and M4 ORFs, suggests all three likely arose through gene duplication events (18, 48). To determine if the M1 antigen is truly a secreted protein with the potential to directly interact with Vβ4⁺ CD8⁺ T cells, we cloned the full-length M1 ORF (with a C-terminal FLAG-epitope tag) into a eukaryotic expression vector and expressed M1 by transient transfection into Cos-1 cells. As predicted, an ~47-kD protein was detected in the transfected culture supernatant after anti-FLAG immunoprecipitation (Fig. 6 A). Expression of a FLAG-tagged version of the MHV68 M3 chemokine-binding protein served as a positive control for secretory transport, whereas a FLAG-tagged MHV68 v-cyclin expression vector resulted in protein expression that was detected only within the whole-cell lysate (Fig. 6 A).

To determine if secreted M1 antigen could directly stimulate Vβ4⁺ CD8⁺ T cells in vitro, cell-free supernatants recovered from Cos-1 cells transfected with either the M1 expression vector, or control expression vectors (M3 and v-cyclin), were used to stimulate splenocytes recovered from mice 4–6 mo after WT MHV68 infection (diagrammed in Fig. 6 B). Stimulation of Vβ4⁺ CD8⁺ T cells was measured using intracellular cytokine (ICC) staining for IFNγ production. Anti-CD3 antibody was used as a nonspecific TCR cross-linking agonist to assess the total capacity for IFNγ production, and elicited robust cytokine levels from Vβ4⁺ CD8⁺ T cells at all times tested (Fig. 6 C). In cultures containing the M1 antigen as a stimulus, a substantial portion (10–20%) of Vβ4⁺ CD8⁺ T cells also produced IFNγ, whereas no activation was elicited by recombinant M3 protein (Fig. 6 C). Importantly, M1-mediated T cell stimulation was lost when recombinant M1 protein was depleted from the supernatant by anti-FLAG immunoprecipitation, indicating that stimulation was specific to the presence of the M1 antigen and not a secondary effect of another soluble factor elicited by M1 expression (Fig. 7 A). Notably, even in the absence of in vitro stimulation, intracellular IFNγ could often be detected within the Vβ4⁺ CD8⁺ T cells from certain infected mice, demonstrating the likelihood that Vβ4⁺ CD8⁺ T cells contribute to persistent IFNγ production in vivo (Fig. 6 C). In contrast to the behavior of the activated Vβ4⁺ CD8⁺ T cell population recovered from WT MHV68-infected mice, recombinant M1 antigen was not capable of stimulating IFNγ production from unexpanded Vβ4⁺ CD8⁺ T cells derived from the spleen of M1.STOP-infected or naive mice in the ICC assay (Fig. S2). The incapacity of M1 to rapidly induce IFNγ production

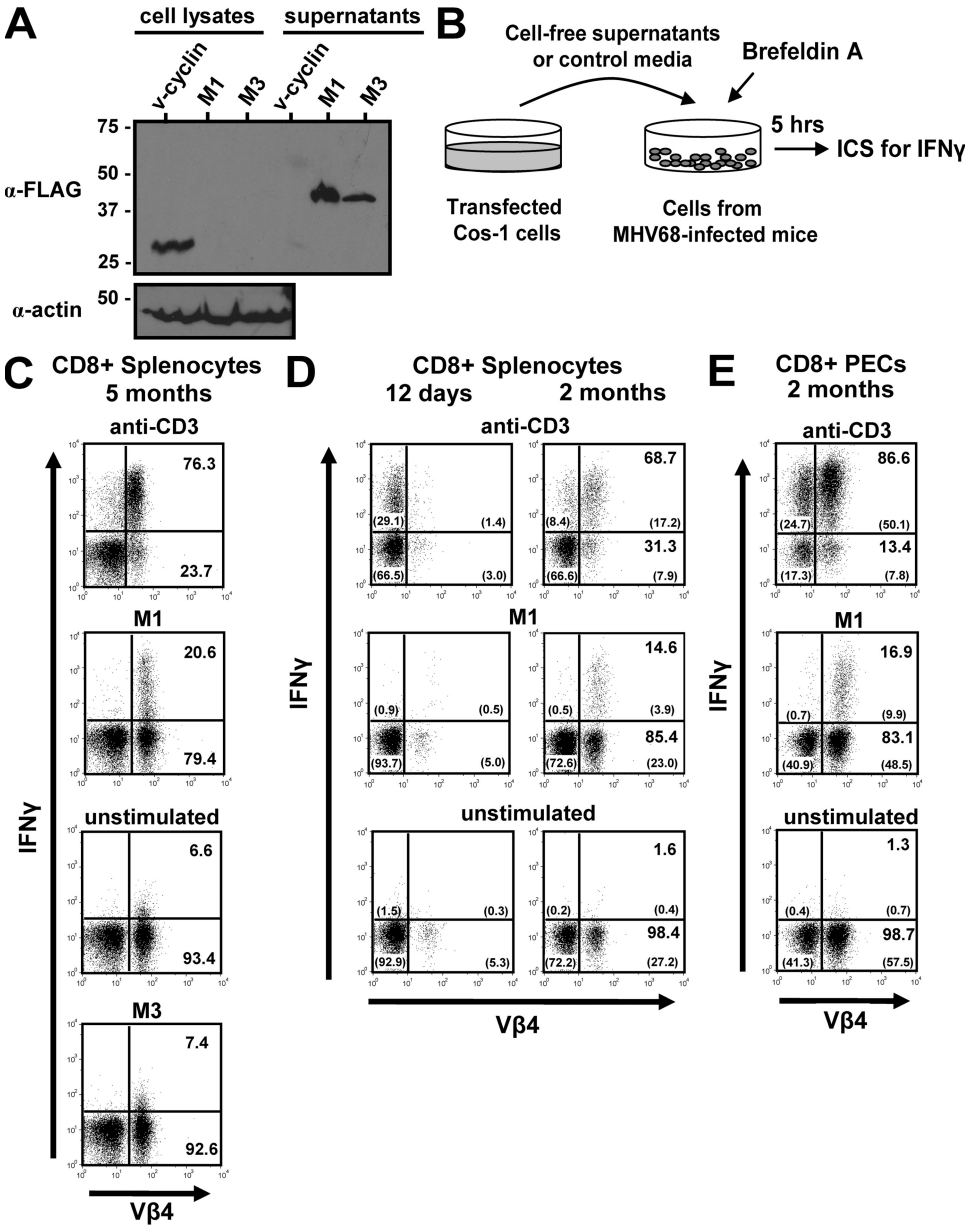

Figure 6. The M1 ORF encodes a 45-kD secreted protein that is capable of stimulating MHV68-induced Vβ4⁺ CD8⁺ T cells. (A) Cos-1 cells were transiently transfected with M1 and M3 expression constructs containing C-terminal FLAG epitopes. Whole-cell lysates and cell supernatants were immunoprecipitated and detected with anti-FLAG antibody. (B) Schematic diagram of experimental design for T cell stimulation. Supernatants from Cos-1–transfected cells containing M1 and M3 recombinant protein were compared with complete media with and without 1 μg/ml anti-CD3, all supplemented with Brefeldin A, for the ability to stimulate primary Vβ4⁺ CD8⁺ T cells from infected C57BL/6 mice as determined by ICC staining for IFNγ. (C) IFNγ production elicited by the indicated stimuli from CD8⁺ splenocytes at 4–6 mo after infection. Note that the extent of background IFNγ production among unstimulated Vβ4⁺ CD8⁺ T cells exhibited mouse-to-mouse variation, but was repeatedly higher then Vβ4⁻ cells and was most readily detected at a 1:100 dilution of Brefeldin A (GolgiPlug). Numeric values are given for the proportion of Vβ4⁺ CD8⁺ cells (right quadrants) only. (D) IFNγ production elicited by the indicated stimuli from CD8⁺ splenocytes at 12 d and 2 mo after infection. Numeric values for the proportion of Vβ4⁺ cells (right quadrants only) are given for the 2-mo time point in larger font, and the total proportion of CD8⁺ cells in each quadrant are given for both time points in parentheses. (E) IFNγ production elicited by the indicated stimuli from CD8⁺ PECs at 2 mo after infection. Numeric values are reported as in D. In all panels, plots are representative of two or more independent experiments, each containing 2–3 mice.

from naive Vβ4⁺ T cells ex vivo was not unexpected, as primary Vβ4⁺ CD8⁺ T cell activation during infection requires costimulation; even potent CD3 cross-linking was incapable of stimulating IFNγ among naive T cells in the same assay.

To compare the capacity of recombinant M1 to stimulate T cells that express Vβ4⁺ TCR alongside other Vβ elements, we examined primary T cells from various times and anatomical sites after infection. First, T cells from mice 12 d after

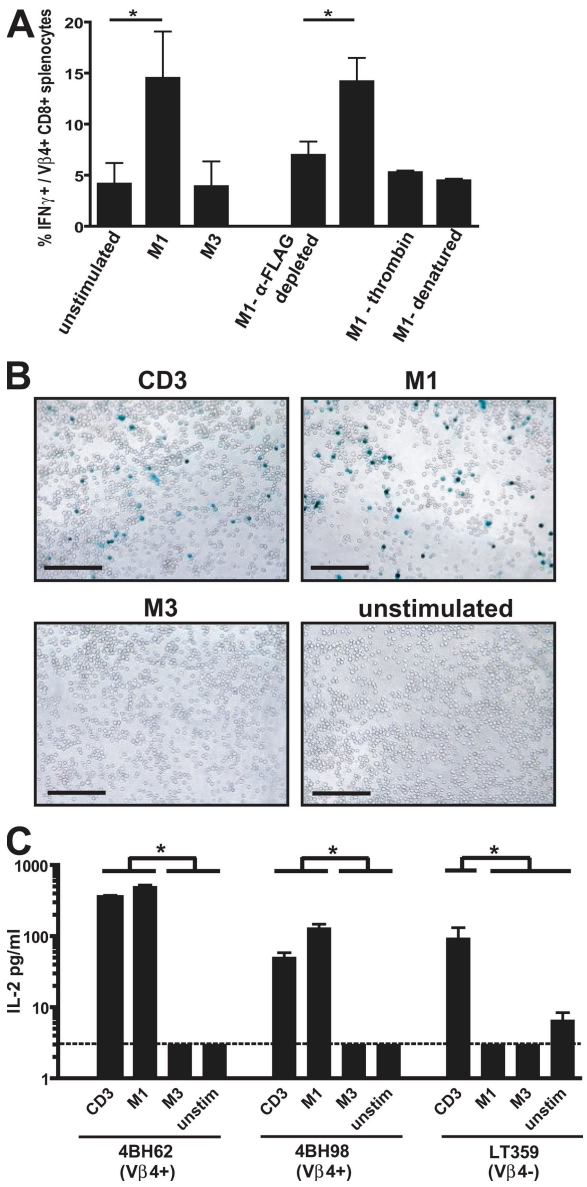

Figure 7. Vβ4⁺ TCR stimulation by M1 requires intact protein and is independent of professional antigen presentation. (A) Histograms quantifying the percentage of Vβ4⁺ CD8⁺ splenocytes that produce IFNγ under the indicated condition. M1-containing supernatants were modified in the following manner. Depleted and nondepleted supernatants were immunoprecipitated using anti-FLAG- and IgG-conjugated agarose, respectively. Thrombin-conjugated agarose was used to protease digest recombinant M1, and then enzyme was removed by precipitation and inactivated with protease inhibitors. M1 contains a single predicted thrombin cleavage domain approximately midway through the primary sequence. M1 denaturation was the result of a 10-min incubation at 94°C. Asterisks indicate significantly different values for representative columns ($P < 0.05$). (B) Vβ4⁺ CD8⁺ hybridoma (4BH62) was cultured in isolation from any other cells for 36 h in the presence of M1- and M3-containing supernatants or conditioned supernatants from Cos-1 cells both with and without 1 μg/ml anti-CD3. Cells were fixed, stained with X-gal for LacZ expression, and photographed under an inverted microscope. Bars, 80 μm. (C) ELISA measurements for the concentration of IL-2 in the culture supernatant of each hybridoma line after 36 h stimulation under the indicated conditions, as in part B. The limit of detection is 2 pg/ml. As a control, all supernatants were tested and found below the limit of detection before being used to culture hybridoma lines (not depicted). Error bars denote the SD.

infection (lacking an expanded Vβ4⁺ population) were compared in parallel with those from mice 2 mo after infection. In side-by-side experiments M1 was devoid of any stimulatory activity among the day 12 effector CD8⁺ T cells, which were capable of responding to anti-CD3 treatment, but produced significant up-regulation of IFNγ among the Vβ4⁺ population from latently infected tissues (Fig. 6 D). The same pattern was true of cells from the peritoneal compartment. Recombinant M1 had no influence on effector CD8⁺ T cells present during lytic infection (unpublished data), but exhibited robust activity among Vβ4⁺ cells taken at 2 mo after infection (Fig. 6 E). Importantly, peritoneal cells from latently infected mice offered a comparison of activity among Vβ4⁺ and Vβ4⁻ T cells, which are both capable of expressing IFNγ within the same sample, and, as such, demonstrated that the influence of M1 was absolutely restricted to the Vβ4⁺ population (Fig. 6 E). Thus, under these conditions, M1 is incapable of stimulating conventional CD8⁺ effector T cells generated during lytic infection, and shows specificity for the presence of a Vβ4⁺ TCR upon ex vivo stimulation. The inability of M1 to influence conventional CD8⁺ T cell responses is further supported by data demonstrating that the peak size of an antigen-specific (tetramer-positive) CD8⁺ T cell response to MHV68 does not significantly differ between infection with M1.STOP and WT virus (Fig. S3, available at http://www.jem.org/cgi/content/full/jem.20071135/DC1).

Vβ4⁺ TCR activation by M1 requires a functional protein and is independent of professional antigen presentation

To assess the requirement for functional M1-mediated protein interactions during T cell stimulation, we disrupted native M1 protein structure via either heat denaturation or enzymatic cleavage with thrombin protease (a single predicted thrombin recognition site exists midway through the protein). The loss of T cell stimulation under either condition suggested M1 activity was dependent on properly folded, intact recombinant protein (Fig. 7 A). Furthermore, it indicated that the stimulatory activity is unlikely to result from an M1-derived peptide epitope presented in an MHC-dependent context during the ICC assay. Such a conclusion was also supported by the inability of a proteasome inhibitor (18 μM lactacystin) to diminish Vβ4⁺ CD8⁺ T cell activation mediated by recombinant M1 (unpublished data). From these analyses, we conclude that the intact extracellular M1 antigen is required to induce Vβ4-specific T cell stimulation after MHV68 infection, implicating a mechanism for Vβ-specific TCR engagement in a manner similar to known superantigens.

Second, we examined the capacity of M1 to stimulate MHV68-specific Vβ4⁺ CD8⁺ T cell hybridomas. The hybridoma lines respond to MHV68-infected splenocytes even in the presence of MHC class I and II blocking antibodies or

when infected splenocytes lacking MHC class I expression (β2-microglobulin$^{-/-}$) are used (37). Each hybridoma line (4BH62 and 4BH98) expresses a distinct Vβ4$^+$ TCR of different complementarity-determining region–3 length and contains a β-galactosidase (*LacZ*) reporter gene regulated by the nuclear factor of activated T cells (NF-AT). After 36 h of stimulation in the presence of M1-containing supernatant, a significant number of the Vβ4$^+$ CD8$^+$ T cell hybridoma cells expressed detectable *LacZ* expression (Fig. 7 B). The number of responding cells was on par with the proportion expressing *LacZ* after anti-CD3 stimulation, whereas no cells were seen to respond to either M3 or mock treatment (Fig. 7 B). Next, interleukin-2 (IL-2) secretion was measured under each condition. A non-Vβ4 CD8$^+$ T cell hybridoma (LT359) derived from a polyoma virus-specific T cell response was used as a control for Vβ-specificity. IL-2 production for each Vβ4$^+$ hybridoma was similar, if not greater, after treatment with M1 as compared with anti-CD3, whereas background levels of IL-2 were undetectable (Fig. 7 C). Notably, the polyoma-specific Vβ4$^-$ hybridoma demonstrated robust IL-2 production in response to anti-CD3 stimulation, but not in response to treatment with M1 (Fig. 7 C). Thus, M1 has the capacity to induce signaling through multiple TCR clones in a Vβ4-specific manner in the absence of professional antigen-presenting cells or any other viral gene product.

DISCUSSION

The salient features of the Vβ4$^+$ CD8$^+$ T cell response have been interpreted as evidence for an unconventional viral superantigen, although no such molecule has previously been identified. Our results demonstrate that the MHV68 M1 antigen is necessary for the Vβ4$^+$ CD8$^+$ T cell response to occur in vivo and is sufficient to induce Vβ4$^+$ TCR signaling in vitro, conclusively demonstrating that M1 is the viral determinant responsible for this immune reaction. M1 activity has several features in common with superantigen-mediated T cell activation, including the following: (a) that it occurs to varying degrees in multiple MHC backgrounds, (b) is independent of professional antigen presentation, and (c) is the result of functional protein–protein interactions that occur specifically with cells bearing a Vβ4$^+$ TCR. The consequences of the superantigen-like response determine several features of MHV68 infection. Upon activation, Vβ4$^+$ CD8$^+$ T cells from C57BL/6 mice appear to suppress reactivation from some populations of latently infected cells, which correlates with the capacity to express high levels of IFNγ, a known inhibitor of MHV68 reactivation from macrophages (Fig. 8) (7, 8). Furthermore, in animals unable to regulate reactivation via IFNγ signaling (IFNγR$^{-/-}$), the presence of the activated Vβ4$^+$ CD8$^+$ T cell population is associated with severe inflammation and fibrotic scarring of multiple tissues (Fig. 8).

Mechanism of M1 action

Identification of a viral molecule that stimulates CD8$^+$ T cells in a manner reminiscent of a superantigen is a novel discovery in regard to both microbial pathogenesis and T cell receptor signaling. Superantigens are expressed by other viruses, including the mouse mammary tumor virus, mls antigen, and Rabies virus nucleocapsid; superantigen activity is implicated in EBV, human cytomegalovirus (HCMV), and herpesvirus saimiri infection (49–54). Like their bacteriological counterparts,

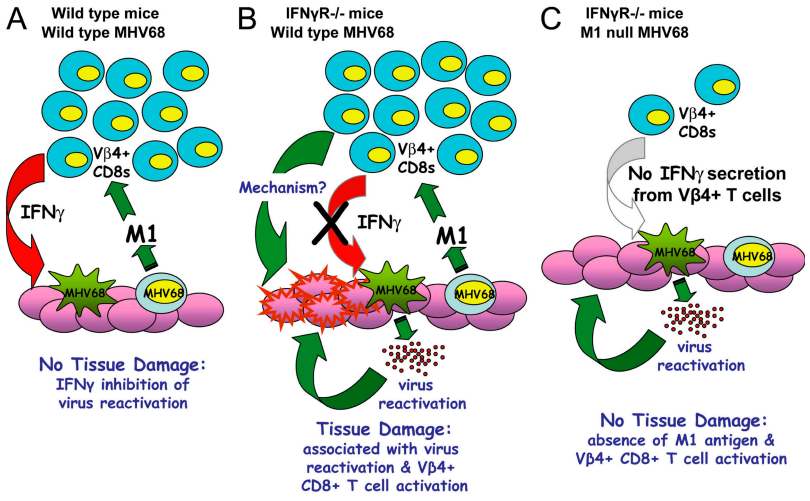

Figure 8. Model for M1 antigen–mediated control of virus reactivation, and association of M1 antigen with the induction of fibrotic disease in IFNγ-unresponsive mice. (A) Infection of WT C57BL/6 mice elicits a strong Vβ4$^+$ CD8$^+$ T cell response via stimulation by soluble M1. Subsequent virus reactivation events lead to limited Vβ4$^+$ CD8$^+$ T cell activation, IFNγ production, and the suppression of virus reactivation from specific latently infected cell populations (i.e., macrophages). (B) MHV68 infection in IFNγR$^{-/-}$ mice leads to virus reactivation and persistent virus replication. In this scenario, the failure of infected cells to respond to IFNγ-mediated suppression of virus reactivation leads to hyperactivation of the expanded Vβ4$^+$ CD8$^+$ T cell population, resulting in tissue damage by an unknown mechanism (see Discussion). (C) Infection of IFNγ-unresponsive mice with M1-null MHV68 fails to elicit expansion or activation of Vβ4$^+$ CD8$^+$ T cells, and no tissue damage is observed in this setting, even though there is ongoing virus reactivation and replication, as shown in Fig. 1 D.

the known viral superantigens mediate bridging interactions between MHC class II molecules and Vβ segments of the TCR β-chain on $CD4^+$ T cells (55, 56). In the case of M1, both its specificity for $CD8^+$ cells and its apparent independence of MHC class Ia interactions are intriguing features that require further elucidation. Importantly, a recent study demonstrated that bacterial superantigens are capable of TCR stimulation independent of lck-mediated phosphorylation events associated with T cell coreceptor engagement (57). If conventional superantigen activity functions independent of MHC-specificity imparted by CD4 and/or CD8 coreceptors, a novel superantigen might circumvent classical MHC–TCR interactions entirely. Indeed, the cumulative data on $V\beta4^+$ $CD8^+$ T cell activation support this idea. We confirmed reports that $V\beta4^+$ $CD8^+$ T cell activation occurs in mice lacking β2m-dependent class I MHC expression (unpublished data), and $V\beta4^+$ $CD8^+$ T cell hybridoma activation in the presence of MHC class I and II neutralizing antibodies also argues against a critical role for antigen-presenting molecules in the MHV68-induced response (37, 41). The defective $V\beta4^+$ $CD8^+$ T cell response in MHV68-infected MHC class II–deficient mice is likely caused by the absence of $CD4^+$ T cells—a known requirement for $V\beta4^+$ $CD8^+$ T cell expansion in vivo (32, 36, 58). Therefore, M1 may signal through an interaction with a nonclassical MHC class Ib molecule, or perhaps mediate some novel manipulation of TCR and CD8 ligation that is entirely MHC independent. Further study of the molecular interactions involved in M1-mediated TCR activation will shed light on such possibilities.

$V\beta4^+$ $CD8^+$ T cell–mediated control of infection

M1-mediated stimulation of $V\beta4^+$ $CD8^+$ T cells promotes their continual proliferation, potent effector cytokine production, and long-term capacity to suppress viral reactivation apparently through IFNγ production. These findings support a less appreciated role for noncytolytic $CD8^+$ T cell function mediated by effector cytokines. The mechanism by which IFNγ controls reactivation is not fully characterized, but even short-course IFNγ blockade in vivo results in a greatly increased frequency of MHV68 reactivation from PECs after explant (7). Likewise, the increased frequency of PECs that reactivate in culture after an M1-null virus infection is likely the result of the relatively poor IFNγ response elicited in the absence of $V\beta4^+$ $CD8^+$ T cell expansion. Obviously, the potential sources of IFNγ during infection are not limited to $V\beta4^+$ $CD8^+$ T cells. Indeed, the frequency of reactivation in the absence of M1 is less exaggerated than that of WT virus in mice lacking IFNγ or its receptor (59). $CD4^+$ T cells regulate MHV68 infection in an IFNγ-dependent manner, whereas NK cells, although likely candidates, do not appear to regulate MHV68 infection (60–62).

Stimulation by M1 does not appear to promote anti-MHV68 cytolytic activity from $V\beta4^+$ $CD8^+$ T cells in vivo, because the frequency of latently infected cells does not decrease in their presence. Blackman et al. reported that $V\beta4^+$ $CD8^+$ T cells kill targeted cells in a peptide-nonspecific manner, but the in vivo relevance of this activity is not known (33). The same study reported $V\beta4^+$ T cell depletion has no significant impact on viral genome load or reactivation from splenocytes, specifically; this is a conclusion that is consistent with our own. It should be noted, however, that our attempt to perform a similar depletion protocol using the same monoclonal antibody (KT4, the only Vβ4-specific monoclonal antibody available to our knowledge) was unsuccessful. Treatment rendered the $V\beta4^+$ population undetectable by flow cytometry with the same monoclonal antibody, but no change in IFNγ production was evident in anti-Vβ4–treated versus isotype-control–treated mice (Fig. S4, available at http://www.jem.org/cgi/content/full/jem.20071135/DC1). These data argue that use of the KT4 antibody masks detection with the same monoclonal species, but does not effectively deplete the $V\beta4^+$ $CD8^+$ T cell population during MHV68 infection. Thus, analyses with an M1 mutant virus may be the most reliable method for evaluating the functional consequences of this T cell response.

The capacity of $V\beta4^+$ $CD8^+$ T cells to maintain functionality over a period of months, and perhaps years, in spite of their continual activation, is in apparent contrast to many antigen-specific T cell responses in other well-known persistent viral infections. Chronic lymphocytic choriomeningitis virus, hepatitis C virus, and simian and human immunodeficiency virus infections eventually result in the development of $CD8^+$ T cell responses with "exhausted" characteristics, including poor proliferative potential, limited effector cytokine production (i.e., TNF-α), and reduced cytolytic activity. This phenomenon, which is thought to result from chronic exposure to viral antigen, is mediated by the PD-1 surface receptor and contributes to the failure to control viral infection in certain cases (63). $V\beta4^+$ $CD8^+$ T cells exhibit the opposite profile, as they fail to express PD-1 on their surface, maintain production of effector cytokines, and exhibit long-term control of persistent virus reactivation. Such a comparison implies that either a relatively low level of activity is required for $V\beta4^+$ $CD8^+$ T cells to control reactivation (i.e., no cytolytic activity and limited cytokine production), or that their activation state is distinct from classical antiviral responses. T cell responses to other latent herpesviruses (i.e., EBV and human or mouse cytomegalovirus) have been described which do not exhibit the hallmarks of exhaustion, but during latency the extent of conventional antigen exposure is presumably low. The paradox of the $V\beta4^+$ $CD8^+$ T cell response to MHV68 is how such a large and activated $CD8^+$ T cell response maintains its size, status, and functional activity. Understanding the mechanisms by which M1 induces persistent $V\beta4^+$ $CD8^+$ T cell activation may provide insight into TCR signaling mechanisms by which more durable and effective T cell responses can be generated against chronic viruses.

Latency as a requirement for the $V\beta4^+$ $CD8^+$ T cell response

Although transcription of the M1 ORF occurs during both lytic and latent MHV68 infection, in B cells as well as non-B cells, the ability of MHV68 to establish latency in B cells is

critically important for Vβ4$^+$ CD8$^+$ T cell activation (30, 36–38, 64, 65). The strict requirement for M1 expression and B cell latency in the Vβ4$^+$ CD8$^+$ T cell response could be explained by several scenarios. The M1 ORF may be differentially regulated by alternative promoter usage during B cell infection, similar to the manner in which EBV modulates different latent transcriptional programs (66). Alternatively, naive Vβ4$^+$ CD8$^+$ T cells may require M1-expressing cells to reside within a specific microenvironment or lymphoid tissue during primary stimulation, as is true for antigen-bearing cells during conventional T cell stimulation. Migration of infected B cells might be required in this latter scenario. Regardless, M1 provides a unique T cell–dependent mechanism to elicit host cytokine expression and subsequently inhibit virus reactivation from non-B cell reservoirs that may be less amenable to long term maintenance of the latent viral genome.

In addition, such an extraordinary T cell response could explain several interesting immunological features of MHV68 latency, such as why: (a) B cell–deficient mice fail to regulate persistent reactivation, but when reconstituted with B cells that do not recognize viral antigen control is recovered in a T cell–dependent manner (64, 67); (b) CD8$^+$ T cells are capable of controlling virus reactivation even in the absence of classical MHC class Ia molecules (41); (c) MHV68 infection results in enhanced lymphoproliferative disease in the absence of M1 in some settings (68); and (d) M1 is required for MHV68 to promote CD8$^+$ T cell–mediated transplant rejection in latently infected recipients (unpublished data). The possibility that the Vβ4$^+$ CD8$^+$ T cell population is playing a role in each of these phenomena is consistent with the available data, and we suggest that this long underappreciated T cell response could affect several of these interesting features of MHV68 latency.

Herpesviruses and immune dysfunction

MHV68-associated fibrosis and vasculitis are proposed as models of several poorly understood clinical pathologies, implicating latent or unknown herpesviruses in the pathogenesis of human disease. Although these MHV68-induced pathologies do not have perfect clinical correlates to known human gammaherpesvirus-associated diseases, they do provide proof that dysregulated immune function during persistent infection can produce devastating disease, the type that could be misinterpreted as purely autoimmune or idiopathic phenomenon if infection goes undetected. Fibrosis associated with MHV68 requires persistent viral replication (11, 15), but we show that persistence is insufficient in the absence of M1 expression and an activated Vβ4$^+$ CD8$^+$ T cell response. The relationship between persistent infection, T cells, and other cell types implicated in MHV68-induced fibrosis (such as macrophages) presents a complex dynamic that will require careful dissection (10). Pathological changes in Vβ4$^+$ CD8$^+$ T cell activity could result from their own lack of IFNγ responsiveness. Alternatively, the chronic inflammatory environment in persistently infected IFNγR$^{-/-}$ mice may enhance Vβ4$^+$ CD8$^+$ T cell activation, above and beyond the "priming" that occurs via M1 stimulation. We propose that Vβ4$^+$ CD8$^+$ T cells might exhibit aberrant cytolytic activity and bystander killing precisely because reactivating cells fail to respond to IFNγ, as diagramed in Fig. 7. Elucidating a role for M1 in T cell activation will aid further attempts to understand the dynamic at work in this process.

Is there any evidence for superantigen function during human gammaherpesvirus infection or disease? EBV infection induces expression of a human endogenous retroviral superantigen (HERV-K18) encoded by the host cell (69). The significance of such superantigen activation on EBV pathogenesis is unclear (70, 71). T cell activation after EBV infection is significantly altered during IM, particularly in patients with a genetic deficiency of the lymphocyte signaling regulator SLAM-associated protein (SAP or *SH2D1A*) (72). These individuals develop a fatal syndrome known as X-linked lymphoproliferative disease, presumably as a result of failure to properly regulate antiviral immune responses. This syndrome has been modeled using chronic viral infection of SAP-deficient mice (73). Because the Vβ4$^+$ CD8$^+$ T cell response has been proposed as a model for IM, it should be noted that the extent of Vβ4$^+$ proliferation after MHV68 infection of SAP-deficient mice is immensely exaggerated (80–90% of all CD8$^+$ T cells in circulation are Vβ4$^+$ in some animals), and like their human counterparts, these mice develop an immune-mediated pathology in multiple organs (74, 75). This raises the question of whether, in both human and murine gammaherpesvirus infection, superantigen-like activity is involved in promoting inflammatory disease. Further studies of these and other pathologies may identify new roles for microbial immunomodulatory molecules in presumptively autoimmune or chronic inflammatory processes.

MATERIALS AND METHODS

Viruses and tissue culture. Viral stocks were generated by transfecting WT and mutant MHV68, cloned as a bacterial artificial chromosome (BAC), into Vero-Cre cells to excise BAC sequence by Cre-mediated recombination (76, 77). NIH 3T12 cells and mouse embryonic fibroblasts (MEFs) were maintained in Dulbecco's modified Eagle's medium, supplemented with 10% FCS, 100 U of penicillin per ml, 100 mg of streptomycin per ml, and 2 mM L-glutamine (CMEM). MEFs were obtained from C57BL/6 mouse embryos as previously described (78). Vero-Cre cells were a gift from D. Leib (Washington University, St. Louis, MO), and they were passaged in CMEM supplemented with 300 1 μg/ml g/ml Hygromycin B.

Mice and infections. C57BL/6, BALB/c, and IFNγR$^{-/-}$ mice (B6.129S7-*Ifngr*^{tm1Agt}/J) were purchased from The Jackson Laboratory and bred in Emory University's animal facilities. Intranasal and intraperitoneal inoculations were performed in a total volume of 20 μl and 400 μl, respectively, diluted in CMEM accordingly. Mice were used between 8–14 wk of age and placed under isoflurane anesthesia before infection and sacrifice by cervical dislocation. All protocols for animal studies were approved by the Institutional Animal Use and Care Committee of Emory University.

Histopathology and immunohistochemical slide preparation. Organs were harvested and fixed overnight in 10% buffered formalin. 7-μm sections from paraffin-embedded tissues were cut and stained with hematoxylin and eosin by the Veterinary Pathology office at Emory University. Images were acquired with an AXIO Imager.A1 microscope and an Axiocam MRc5 (Carl Zeiss, Inc.).

Immunohistochemistry was performed on fresh frozen lung sections. Mounted serial sections were blocked before staining for Vβ4 TCR and CD8β (both rat anti–mouse; AbD Serotec) or normal rat IgG (Santa Cruz Biotechnology) as a negative control. Secondary biotinylated rabbit anti–rat (Dako) was used before quenching endogenous peroxidase activity with 0.3% H_2O_2 and exposure to a streptavidin/horseradish peroxidase conjugate and diaminobenzidine (Vector Laboratories) as chromogen.

Flow cytometry and intracellular cytokine staining. Single-cell suspensions resuspended in PBS with 1–2% FCS (FACS Buffer). For staining, 1–2 × 10^6 cells were Fc-blocked with 1:50 dilution of anti-FcγII/IIIR (2.4G2) before staining with each of the following monoclonal antibodies: Vβ4 TCR (KT4), CD11a (M17/4), CD44 (IM7), CD62L (MEL-14), CD25 (7D4), CD69 (H1.2F3), CD127 (SB/199), PD-1 (J43), NKG2A (16A11; BD Biosciences), and CD8α (CT-CD8a; Caltag Laboratories). Various fluorophore conjugates for each monoclonal species were used in different panels depending on the availability of each conjugated activation marker. For BrdU analysis, mice were given fresh BrdU daily in their drinking water (0.8 mg/ml) for 8 d starting 4 mo after infection. Intracellular staining used a BrdU flow kit (BD Biosciences) and followed the manufacturer's instructions. Stimulation of cytokine production entailed culturing splenocytes for 4–6 h in the presence of a 1:100–1:1,000 dilution of GolgiPlug (BD Biosciences) in fresh CMEM with or without the addition of either 1 μg/ml of anti-CD3 monoclonal (145-2C11; BD Biosciences). The stimulatory activity of each recombinant protein was assessed by the addition of GolgiPlug alone to the supernatant from Cos-1 cells 48 h after transfection, and then using the supernatant for splenocyte culture. After stimulation, surface staining was performed as above, followed by cell permeabilization and fixation (Cytofix/Cytoperm kit; BD Biosciences) and intracellular staining for Vβ4 TCR (required because of surface downmodulation during stimulation), IFNγ (XMG1.2), and TNF-α. Data were collected on a FACSCalibur (BD Biosciences) and analyzed using FlowJo software (Tree Star, Inc.).

Plaque assays. Plaque assays were performed as previously described (18), with the following alterations. Tissues were weighed before freezing in 1 ml CMEM, and then thawed and homogenized by mechanical disruption with 1.0 mm zirconia/silica beads in a Mini-Beadbeater 8 (Biospec Products). 10-fold dilutions made in CMEM were plated onto monolayers of 2 × 10^5 NIH 3T12 fibroblasts. Samples were overlaid with 5 ml of 2% methylcellulose in CMEM, and after 7 d, plaques were counted by microscopic examination. Plaque titers were normalized per gram of tissue, and the limit of detection for this assay is based on detection of 5 PFU per 0.1 g of tissue.

Limiting dilution ex vivo reactivation assay. Detection of MHV68 reactivation from latency was performed as previously described (67). In brief, cells were plated in a series of twofold dilutions, starting at 10^5 cells per well, onto MEF monolayers in 96-well tissue culture plates. After 21 d, wells were scored microscopically for the presence of CPE. To detect preformed infectious virus, parallel samples were subjected to mechanical disruption as previously described, killing >99% of cells. Disrupted cells were plated in a similar series of twofold dilutions.

Limiting dilution nested PCR detection of MHV68 genome-positive cells. We determined the frequency of cells containing MHV68 genome using a previously described nested PCR assay (LD-PCR) with approximately single-copy sensitivity to detect gene 50 of MHV68 (67). In brief, cells were counted and resuspended in an isotonic solution, and diluted in a background of 10^4 uninfected NIH 3T12 cells. After overnight lysis of cells with proteinase K, two rounds of nested PCR were performed on each sample. Products were analyzed by ethidium bromide staining of a 2% agarose gel. To quantitate PCR sensitivity, 10, 1, or 0.1 copies of a gene 50 containing plasmid (p*Bam*H I N) were diluted into a background of 10^4 uninfected cells.

Generating recombinant M1.STOP virus. WT MHV68 BAC DNA was mutagenized by allelic exchange in Rec-A–positive *Escherichia coli*, as previously described (76), with the following modifications. A DNA fragment containing an M1 kanamycin insertion (M1.Kan) was generated by incorporating a novel Avr II restriction site into position 2153 (GenBank accession no. NC_001826) of the M1 ORF with overlap extension PCR. The kanamycin resistance cassette from the Xbal fragment of pCP15 into this site was then subcloned into the AvrII site. The resulting M1.Kan construct was transfered into the pGS284 suicide vector and allelic exchange was performed with the WT MHV68 BAC to generate a kanamycin-resistant BAC in which antibiotic resistance was linked to the M1 ORF (M1.Kan BAC). The M1.STOP mutation, as shown in Fig. 2 C, was also cloned by overlap extension PCR, incorporating two translational termination codons, a single base pair downstream frameshift, and a novel Acl I site into coordinates 2363 through 2373. After sequence confirmation, the M1.STOP allele was cloned into pGS284, allowing allelic exchange to be performed with M1.Kan BAC to exchange the discrete stop mutation for the Kan insertion. M1.STOP BAC was identified by replica plating for the loss of kanamycin resistance, and the entire region was sequenced to confirm fidelity. Genomic integrity of all recombinant BACs was confirmed by Southern blot (Fig. S5, available at http://www.jem.org/cgi/content/full/jem.20071135/DC1). M1.STOP viral stocks were generated as described.

Protein expression and detection. M1 coding sequence (genomic coordinates 2023–3285) was PCR amplified from MHV68 BAC DNA, incorporating a BamHI restriction site and a Kozac sequence immediately upstream of the translational start site and a XhoI restriction site immediately downstream of the last codon. Primer sequences were the following: 5′-TCGAACGGATCCGCCGCCATGCAGCTGGCCACCTTATG-3′ and 5′-GGTTGCCTCGAGGGACTGCTGCCCAGGAAAAAT-3′. PCR products were cloned in-frame with the C-terminal FLAG epitope using the BamHI and XhoI sites contained in the pCMV-Tag4B mammalian expression vector (Stratagene) and sequenced for fidelity. The M3 expression vector was generated in an identical manner, using primer sequences that correspond to genomic coordinates 6060–7277. The v-cyclin expression vector was generated by cloning sequence corresponding to genomic coordinates 102,423–103,181 into pCMV-Tag2B (Stratagene).

Expression vectors were transfected into Cos-1 cells using TransIT-LT1 Reagent (Mirus), per the manufacturer's instructions. After 48 h, transfected cell supernatants were removed and immunoprecipitated overnight using 30 μl anti-FLAG M2-agarose affinity gel (Sigma-Aldrich). Whole-cell lysates were prepared by the addition of E1A lysis buffer (50 mM Hepes, pH 7.2, 250 mM NaCl, 2 mM EDTA, and 0.1% NP-40). Cell lysates and immunoprecipitates were denatured and separated by 10% SDS-PAGE and transferred to nitrocellulose membrane. Nitrocellulose was blocked for 1 h at room temperature, immunoblotted overnight at 4°C with anti-FLAG M2-peroxidase–conjugated antibody (Sigma-Aldrich), and antibody was detected using ECL Western Blot Analysis System (GE Healthcare).

Hybridoma stimulation. $Vβ4^+$ $CD8^+$ hybridomas (4BH62 and 4BH98) were gifts from M. Blackman (Trudeau Institute, Saranac lake, NY), and the polyoma-specific Vβ4-$CD8^+$ T cell hybridoma (LT359) was supplied by A. Lukacher (Emory University, Atlanta, GA). Notably, each line was generated from the fusion of mouse splenocytes with the same hybridoma fusion partner, BWZ.36/CD8α (37). $Vβ4^+$ lines were maintained in Eagle's minimum essential media supplemented with 8.5% FCS and 7.25% tumor cocktail (Eagle's minimum essential media with 75 ml of 10× essential aa, 140 ml of 100× nonessential aa, 100 mM sodium pyruvate, 2 mM L-glutamine, and 7.5 g dextrose/liter, and then pH adjusted to 7.0 with sodium hydroxide before addition of 8.5 g sodium bicarbonate, 500 mg gentamycin, 600 mg penicillin, 1 g streptomycin, and 34 μl of 2-β-mercaptoethanol [βME] per liter). LT359 was maintained in CMEM supplemented with sodium pyruvate, nonessential aa, and βME at the same concentrations indicated in the aforementioned tumor cocktail. During stimulation, 10^5 hybridoma cells were cultured for 24–36 h in flat-bottom, 96-well plates, in the presence of

Cos-1–conditioned supernatants. After stimulation, supernatants were removed and analyzed for the presence of IL-2 by ELISA (BD Biosciences) according to the manufacturer's instructions. LacZ expression was detected by washing cells with PBS, fixing with cold 2% formaldehyde/0.2% glutaraldehyde for 5 min, washing again, and finally staining with the addition of 50 μl of PBS containing 5 mM potassium ferrocyanide, 5 mM potassium ferricyanide, 2 mM $MgCl_2$, and 1 mg/ml of 5-bromo-4-chloro-3-indolyl β-D-galactopyranoside (X-Gal). Cells were incubated for an additional 6–12 h at 37° before being photographed with an inverted tissue culture microscope (Carl Zeiss, Inc.).

Antibody depletion. The KT4 rat hybridoma cell line was a gift from G. Deepe (University of Cincinnati, Cincinnati, OH). The SFR-DR5, IgG2b isotype control–producing rat hybridoma was a gift of E. Barton (Purdue University, West Lafayette, IN). Both cell lines were grown in serum-free hybridoma media (Invitrogen) supplemented with 100 U of penicillin and 100 mg of streptomycin per ml (SFM), using a two-compartment bioreactor (Integra Biosciences) to generate concentrated, serum-free, and cell-free antibody preparations. The relative concentration of each monoclonal species was measured by enzyme-linked immunosorbent assay (ELISA) for total rat IgG2b (Bethyl Laboratories). Each antibody was diluted to an equivalent concentration in SFM, and 300 μg was injected intraperitoneally into infected mice every 3 d starting at 32 d after infection. Mice were killed 10 d later and the extent of $V\beta4^+$ T cell depletion was assessed independently by surface staining for Vβ4 TCR and IFNγ production.

Statistical analysis. All data were analyzed using GraphPad Prism software (GraphPad Software). Titer data were compared using an unpaired, two-tailed Student's *t* test to evaluate statistical significance. Histograms denoting the percentage of $V\beta4^+$ $CD8^+$ T cells elicited by each virus in each respective mouse strain represent the mean value ± the SEM from 1–4 individual experiments with 2–5 mice per group. Limiting dilution analyses for the evaluation of latent infection represents pooled data from 2–3 individual experiments containing 4–5 mice per group. Data were subjected to nonlinear regression analysis, and the frequency for reactivation or the detection of a genome-positive cell was found using the Poisson distribution to assume that the cell number at which 63.2% of events were detected corresponded to the occurrence of a single event.

Online supplemental material. Fig. S1 shows the ICC staining results for M1-mediated IFNγ production from WT, M1.STOP-infected, and naive mice. Fig. S2 outlines the attempted Vβ4-depletion regimen and shows the results for both Vβ4 and IFNγ staining from KT4- versus isotype control-treated mice. Fig. S3 shows the diagnostic Southern blot confirming the construction and overall genomic integrity of the M1.STOP BAC. Fig. S4 shows the frequency of antigen-specific (p56/H-$2D^b$) $CD8^+$ T cells elicited by M1.STOP versus WT virus. Fig. S5 shows that both the frequency of MHV68 reactivation and the extent of $V\beta4^+$ $CD8^+$ T cell expansion are independent of viral dose. The online version of this article is available at http://www.jem.org/cgi/content/full/jem.20071135/DC1.

The authors wish to acknowledge Drs. A. Grakoui, A. Lukacher, E. Clambey, and J.C. Forrest for helpful discussions; E. Dessasau III for preparing histological sections; and P. Swanson and E. Torres-González for technical assistance.

This work was supported by National Institutes of Health (NIH) grant R01 CA52004. S.H. Speck is also supported by NIH grants CA58524, CA87650, CA95318, and AI058057.

The authors declare that they have no conflicting financial interests.

Submitted: 4 June 2007
Accepted: 7 February 2008

REFERENCES

1. Knipe, D.M., P.M. Howley, D.E. Griffin, R.A. Lamb, S.E. Straus, M.A. Martin, and B. Roizman, editors. 2007. Fields Virology. Lippincott Williams and Wilkins, Philadelphia.
2. Virgin, H.W., P. Latreille, P. Wamsley, K. Hallsworth, K.E. Weck, A.J. Dal Canto, and S.H. Speck. 1997. Complete sequence and genomic analysis of murine gammaherpesvirus 68. *J. Virol.* 71:5894–5904.
3. McGeoch, D.J., D. Gatherer, and A. Dolan. 2005. On phylogenetic relationships among major lineages of the Gammaherpesvirinae. *J. Gen. Virol.* 86:307–316.
4. Speck, S.H., and H.W. Virgin. 1999. Host and viral genetics of chronic infection: a mouse model of gamma-herpesvirus pathogenesis. *Curr. Opin. Microbiol.* 2:403–409.
5. Virgin, H.W., and S.H. Speck. 1999. Unraveling immunity to gammaherpesviruses: a new model for understanding the role of immunity in chronic virus infection. *Curr. Opin. Immunol.* 11:371–379.
6. Dutia, B.M., C.J. Clarke, D.J. Allen, and A.A. Nash. 1997. Pathological changes in the spleens of gamma interferon receptor-deficient mice infected with murine gammaherpesvirus: a role for CD8 T cells. *J. Virol.* 71:4278–4283.
7. Steed, A.L., E.S. Barton, S.A. Tibbetts, D.L. Popkin, M.L. Lutzke, R. Rochford, and H.W. Virgin. 2006. Gamma interferon blocks gammaherpesvirus reactivation from latency. *J. Virol.* 80:192–200.
8. Steed, A., T. Buch, A. Waisman, and H.W. Virgin. 2007. Gamma interferon blocks gammaherpesvirus reactivation from latency in a cell type-specific manner. *J. Virol.* 81:6134–6140.
9. Ebrahimi, B., B.M. Dutia, D.G. Brownstein, and A.A. Nash. 2001. Murine gammaherpesvirus-68 infection causes multi-organ fibrosis and alters leukocyte trafficking in interferon-gamma receptor knockout mice. *Am. J. Pathol.* 158:2117–2125.
10. Mora, A.L., E. Torres-Gonzalez, M. Rojas, C. Corredor, J. Ritzenthaler, J. Xu, J. Roman, K. Brigham, and A. Stecenko. 2006. Activation of alveolar macrophages via the alternative pathway in herpesvirus-induced lung fibrosis. *Am. J. Respir. Cell Mol. Biol.* 35:466–473.
11. Mora, A.L., E. Torres-Gonzalez, M. Rojas, J. Xu, J. Ritzenthaler, S.H. Speck, J. Roman, K. Brigham, and A. Stecenko. 2007. Control of virus reactivation arrests pulmonary herpesvirus induced fibrosis in IFN{gamma}R deficient mice. *Am. J. Respir. Crit. Care Med.* 175:1139–1150.
12. Mora, A.L., C.R. Woods, A. Garcia, J. Xu, M. Rojas, S.H. Speck, J. Roman, K.L. Brigham, and A.A. Stecenko. 2005. Lung infection with gamma-herpesvirus induces progressive pulmonary fibrosis in Th2-biased mice. *Am. J. Physiol. Lung Cell. Mol. Physiol.* 289:L711–L721.
13. Weck, K.E., A.J. Dal Canto, J.D. Gould, A.K. O'Guin, K.A. Roth, J.E. Saffitz, S.H. Speck, and H.W. Virgin. 1997. Murine gamma-herpesvirus 68 causes severe large-vessel arteritis in mice lacking interferon-gamma responsiveness: a new model for virus-induced vascular disease. *Nat. Med.* 3:1346–1353.
14. Dal Canto, A.J., P.E. Swanson, A.K. O'Guin, S.H. Speck, and H.W. Virgin. 2001. IFN-gamma action in the media of the great elastic arteries, a novel immunoprivileged site. *J. Clin. Invest.* 107:R15–R22.
15. Dal Canto, A.J., H.W. Virgin, and S.H. Speck. 2000. Ongoing viral replication is required for gammaherpesvirus 68-induced vascular damage. *J. Virol.* 74:11304–11310.
16. Clambey, E.T., H.W. Virgin, and S.H. Speck. 2000. Disruption of the murine gammaherpesvirus 68 M1 open reading frame leads to enhanced reactivation from latency. *J. Virol.* 74:1973–1984.
17. Clambey, E.T., H.W. Virgin, and S.H. Speck. 2002. Characterization of a spontaneous 9.5-kilobase-deletion mutant of murine gammaherpesvirus 68 reveals tissue-specific genetic requirements for latency. *J. Virol.* 76:6532–6544.
18. Evans, A.G., N.J. Moorman, D.O. Willer, and S.H. Speck. 2006. The M4 gene of gammaHV68 encodes a secreted glycoprotein and is required for the efficient establishment of splenic latency. *Virology.* 344:520–531.
19. Herskowitz, J., M.A. Jacoby, and S.H. Speck. 2005. The murine gammaherpesvirus 68 M2 gene is required for efficient reactivation from latently infected B cells. *J. Virol.* 79:2261–2273.
20. Jacoby, M.A., H.W. Virgin, and S.H. Speck. 2002. Disruption of the M2 gene of murine gammaherpesvirus 68 alters splenic latency following intranasal, but not intraperitoneal, inoculation. *J. Virol.* 76:1790–1801.
21. Macrae, A.I., E.J. Usherwood, S.M. Husain, E. Flano, I.J. Kim, D.L. Woodland, A.A. Nash, M.A. Blackman, J.T. Sample, and J.P. Stewart. 2003. Murid herpesvirus 4 strain 68 M2 protein is a B-cell-associated

antigen important for latency but not lymphocytosis. *J. Virol.* 77: 9700–9709.
22. van Berkel, V., B. Levine, S.B. Kapadia, J.E. Goldman, S.H. Speck, and H.W. Virgin. 2002. Critical role for a high-affinity chemokine-binding protein in gamma-herpesvirus-induced lethal meningitis. *J. Clin. Invest.* 109:905–914.
23. Townsley, A.C., B.M. Dutia, and A.A. Nash. 2004. The m4 gene of murine gammaherpesvirus modulates productive and latent infection in vivo. *J. Virol.* 78:758–767.
24. Cardin, R.D., J.W. Brooks, S.R. Sarawar, and P.C. Doherty. 1996. Progressive loss of CD8+ T cell-mediated control of a gamma-herpesvirus in the absence of CD4+ T cells. *J. Exp. Med.* 184:863–871.
25. Ehtisham, S., N.P. Sunil-Chandra, and A.A. Nash. 1993. Pathogenesis of murine gammaherpesvirus infection in mice deficient in CD4 and CD8 T cells. *J. Virol.* 67:5247–5252.
26. Husain, S.M., E.J. Usherwood, H. Dyson, C. Coleclough, M.A. Coppola, D.L. Woodland, M.A. Blackman, J.P. Stewart, and J.T. Sample. 1999. Murine gammaherpesvirus M2 gene is latency-associated and its protein a target for CD8(+) T lymphocytes. *Proc. Natl. Acad. Sci. USA.* 96:7508–7513.
27. Liu, L., E.J. Usherwood, M.A. Blackman, and D.L. Woodland. 1999. T-cell vaccination alters the course of murine herpesvirus 68 infection and the establishment of viral latency in mice. *J. Virol.* 73:9849–9857.
28. Usherwood, E.J., D.J. Roy, K. Ward, S.L. Surman, B.M. Dutia, M.A. Blackman, J.P. Stewart, and D.L. Woodland. 2000. Control of gammaherpesvirus latency by latent antigen-specific CD8(+) T cells. *J. Exp. Med.* 192:943–952.
29. Obar, J.J., S.G. Crist, D.C. Gondek, and E.J. Usherwood. 2004. Different functional capacities of latent and lytic antigen-specific CD8 T cells in murine gammaherpesvirus infection. *J. Immunol.* 172:1213–1219.
30. Obar, J.J., S. Fuse, E.K. Leung, S.C. Bellfy, and E.J. Usherwood. 2006. Gammaherpesvirus persistence alters key CD8 T-cell memory characteristics and enhances antiviral protection. *J. Virol.* 80:8303–8315.
31. Stevenson, P.G., G.T. Belz, J.D. Altman, and P.C. Doherty. 1999. Changing patterns of dominance in the CD8+ T cell response during acute and persistent murine gamma-herpesvirus infection. *Eur. J. Immunol.* 29:1059–1067.
32. Tripp, R.A., A.M. Hamilton-Easton, R.D. Cardin, P. Nguyen, F.G. Behm, D.L. Woodland, P.C. Doherty, and M.A. Blackman. 1997. Pathogenesis of an infectious mononucleosis-like disease induced by a murine gamma-herpesvirus: role for a viral superantigen? *J. Exp. Med.* 185:1641–1650.
33. Flano, E., C.L. Hardy, I.J. Kim, C. Frankling, M.A. Coppola, P. Nguyen, D.L. Woodland, and M.A. Blackman. 2004. T cell reactivity during infectious mononucleosis and persistent gammaherpesvirus infection in mice. *J. Immunol.* 172:3078–3085.
34. Doherty, P.C., R.A. Tripp, A.M. Hamilton-Easton, R.D. Cardin, D.L. Woodland, and M.A. Blackman. 1997. Tuning into immunological dissonance: an experimental model for infectious mononucleosis. *Curr. Opin. Immunol.* 9:477–483.
35. Blackman, M.A., E. Flano, E. Usherwood, and D.L. Woodland. 2000. Murine gamma-herpesvirus-68: a mouse model for infectious mononucleosis? *Mol. Med. Today.* 6:488–490.
36. Brooks, J.W., A.M. Hamilton-Easton, J.P. Christensen, R.D. Cardin, C.L. Hardy, and P.C. Doherty. 1999. Requirement for CD40 ligand, CD4(+) T cells, and B cells in an infectious mononucleosis-like syndrome. *J. Virol.* 73:9650–9654.
37. Coppola, M.A., E. Flano, P. Nguyen, C.L. Hardy, R.D. Cardin, N. Shastri, D.L. Woodland, and M.A. Blackman. 1999. Apparent MHC-independent stimulation of CD8+ T cells in vivo during latent murine gammaherpesvirus infection. *J. Immunol.* 163:1481–1489.
38. May, J.S., H.M. Coleman, B. Smillie, S. Efstathiou, and P.G. Stevenson. 2004. Forced lytic replication impairs host colonization by a latency-deficient mutant of murine gammaherpesvirus-68. *J. Gen. Virol.* 85: 137–146.
39. Hardy, C.L., E. Flano, R.D. Cardin, I.J. Kim, P. Nguyen, S. King, D.L. Woodland, and M.A. Blackman. 2001. Factors controlling levels of CD8+ T-cell lymphocytosis associated with murine gamma-herpesvirus infection. *Viral Immunol.* 14:391–402.
40. Hardy, C.L., S.L. Silins, D.L. Woodland, and M.A. Blackman. 2000. Murine gamma-herpesvirus infection causes V(beta)4-specific CDR3-restricted clonal expansions within CD8(+) peripheral blood T lymphocytes. *Int. Immunol.* 12:1193–1204.
41. Braaten, D.C., J.S. McClellan, I. Messaoudi, S.A. Tibbetts, K.B. McClellan, J. Nikolich-Zugich, and H.W. Virgin. 2006. Effective control of chronic gamma-herpesvirus infection by unconventional MHC class Ia-independent CD8 T cells. *PLoS Pathog.* 2:e37.
42. Bowden, R.J., J.P. Simas, A.J. Davis, and S. Efstathiou. 1997. Murine gammaherpesvirus 68 encodes tRNA-like sequences which are expressed during latency. *J. Gen. Virol.* 78(Pt 7):1675–1687.
43. Simas, J.P., R.J. Bowden, V. Paige, and S. Efstathiou. 1998. Four tRNA-like sequences and a serpin homologue encoded by murine gammaherpesvirus 68 are dispensable for lytic replication in vitro and latency in vivo. *J. Gen. Virol.* 79(Pt 1):149–153.
44. Pfeffer, S., A. Sewer, M. Lagos-Quintana, R. Sheridan, C. Sander, F.A. Grasser, L.F. van Dyk, C.K. Ho, S. Shuman, M. Chien, et al. 2005. Identification of microRNAs of the herpesvirus family. *Nat. Methods.* 2:269–276.
45. Kaech, S.M., J.T. Tan, E.J. Wherry, B.T. Konieczny, C.D. Surh, and R. Ahmed. 2003. Selective expression of the interleukin 7 receptor identifies effector CD8 T cells that give rise to long-lived memory cells. *Nat. Immunol.* 4:1191–1198.
46. Moser, J.M., J. Gibbs, P.E. Jensen, and A.E. Lukacher. 2002. CD94-NKG2A receptors regulate antiviral CD8(+) T cell responses. *Nat. Immunol.* 3:189–195.
47. Barber, D.L., E.J. Wherry, D. Masopust, B. Zhu, J.P. Allison, A.H. Sharpe, G.J. Freeman, and R. Ahmed. 2006. Restoring function in exhausted CD8 T cells during chronic viral infection. *Nature.* 439:682–687.
48. van Berkel, V., K. Preiter, H.W. Virgin, and S.H. Speck. 1999. Identification and initial characterization of the murine gammaherpesvirus 68 gene M3, encoding an abundantly secreted protein. *J. Virol.* 73:4524–4529.
49. Lafon, M., M. Lafage, A. Martinez-Arends, R. Ramirez, F. Vuillier, D. Charron, V. Lotteau, and D. Scott-Algara. 1992. Evidence for a viral superantigen in humans. *Nature.* 358:507–510.
50. Dobrescu, D., B. Ursea, M. Pope, A.S. Asch, and D.N. Posnett. 1995. Enhanced HIV-1 replication in V beta 12 T cells due to human cytomegalovirus in monocytes: evidence for a putative herpesvirus superantigen. *Cell.* 82:753–763.
51. Choi, Y., J.W. Kappler, and P. Marrack. 1991. A superantigen encoded in the open reading frame of the 3′ long terminal repeat of mouse mammary tumour virus. *Nature.* 350:203–207.
52. Marrack, P., E. Kushnir, and J. Kappler. 1991. A maternally inherited superantigen encoded by a mammary tumour virus. *Nature.* 349:524–526.
53. Sutkowski, N., T. Palkama, C. Ciurli, R.P. Sekaly, D.A. Thorley-Lawson, and B.T. Huber. 1996. An Epstein-Barr virus-associated superantigen. *J. Exp. Med.* 184:971–980.
54. Yao, Z., E. Maraskovsky, M.K. Spriggs, J.I. Cohen, R.J. Armitage, and M.R. Alderson. 1996. Herpesvirus saimiri open reading frame 14, a protein encoded by T lymphotropic herpesvirus, binds to MHC class II molecules and stimulates T cell proliferation. *J. Immunol.* 156:3260–3266.
55. Moza, B., A.K. Varma, R.A. Buonpane, P. Zhu, C.A. Herfst, M.J. Nicholson, A.K. Wilbuer, N.P. Seth, K.W. Wucherpfennig, J.K. McCormick, et al. 2007. Structural basis of T-cell specificity and activation by the bacterial superantigen TSST-1. *EMBO J.* 26:1187–1197.
56. Mottershead, D.G., P.N. Hsu, R.G. Urban, J.L. Strominger, and B.T. Huber. 1995. Direct binding of the Mtv7 superantigen (Mls-1) to soluble MHC class II molecules. *Immunity.* 2:149–154.
57. Bueno, C., C.D. Lemke, G. Criado, M.L. Baroja, S.S. Ferguson, A.K. Rahman, C.D. Tsoukas, J.K. McCormick, and J. Madrenas. 2006. Bacterial superantigens bypass Lck-dependent T cell receptor signaling by activating a Galpha11-dependent, PLC-beta-mediated pathway. *Immunity.* 25:67–78.
58. Flano, E., D.L. Woodland, and M.A. Blackman. 1999. Requirement for CD4+ T cells in V beta 4+CD8+ T cell activation associated with latent murine gammaherpesvirus infection. *J. Immunol.* 163:3403–3408.
59. Tibbetts, S.A., L.F. van Dyk, S.H. Speck, and H.W. Virgin. 2002. Immune control of the number and reactivation phenotype of cells latently infected with a gammaherpesvirus. *J. Virol.* 76:7125–7132.

60. Sparks-Thissen, R.L., D.C. Braaten, K. Hildner, T.L. Murphy, K.M. Murphy, and H.W.t. Virgin. 2005. CD4 T cell control of acute and latent murine gammaherpesvirus infection requires IFNgamma. *Virology*. 338:201–208.
61. Sparks-Thissen, R.L., D.C. Braaten, S. Kreher, S.H. Speck, and H.W. Virgin. 2004. An optimized CD4 T-cell response can control productive and latent gammaherpesvirus infection. *J. Virol.* 78:6827–6835.
62. Usherwood, E.J., S.K. Meadows, S.G. Crist, S.C. Bellfy, and C.L. Sentman. 2005. Control of murine gammaherpesvirus infection is independent of NK cells. *Eur. J. Immunol.* 35:2956–2961.
63. Sharpe, A.H., E.J. Wherry, R. Ahmed, and G.J. Freeman. 2007. The function of programmed cell death 1 and its ligands in regulating autoimmunity and infection. *Nat. Immunol.* 8:239–245.
64. McClellan, K.B., S. Gangappa, S.H. Speck, and H.W. Virgin. 2006. Antibody-independent control of gamma-herpesvirus latency via B cell induction of anti-viral T cell responses. *PLoS Pathog.* 2:e58.
65. Marques, S., S. Efstathiou, K.G. Smith, M. Haury, and J.P. Simas. 2003. Selective gene expression of latent murine gammaherpesvirus 68 in B lymphocytes. *J. Virol.* 77:7308–7318.
66. Rickinson, A.B., and E. Kieff. 2007. Epstein-Barr virus. *In* Fields Virology. D.M. Knipe and P.M. Howley, editors. Lippincott Williams and Wilkins, Philadelphia. pp. 2655–2700.
67. Weck, K.E., S.S. Kim, H.I. Virgin, and S.H. Speck. 1999. B cells regulate murine gammaherpesvirus 68 latency. *J. Virol.* 73:4651–4661.
68. Tarakanova, V.L., F. Kreisel, D.W. White, and H.W. Virgin. 2007. Murine gammaherpesvirus 68 genes both induce and suppress lymphoproliferative disease. *J. Virol.* 82:1034–1039.
69. Sutkowski, N., B. Conrad, D.A. Thorley-Lawson, and B.T. Huber. 2001. Epstein-Barr virus transactivates the human endogenous retrovirus HERV-K18 that encodes a superantigen. *Immunity*. 15:579–589.
70. Sutkowski, N., G. Chen, G. Calderon, and B.T. Huber. 2004. Epstein-Barr virus latent membrane protein LMP-2A is sufficient for transactivation of the human endogenous retrovirus HERV-K18 superantigen. *J. Virol.* 78:7852–7860.
71. Tai, A.K., M. Lin, F. Chang, G. Chen, F. Hsiao, N. Sutkowski, and B.T. Huber. 2006. Murine Vbeta3+ and Vbeta7+ T cell subsets are specific targets for the HERV-K18 Env superantigen. *J. Immunol.* 177:3178–3184.
72. Ma, C.S., K.E. Nichols, and S.G. Tangye. 2007. Regulation of cellular and humoral immune responses by the SLAM and SAP families of molecules. *Annu. Rev. Immunol.* 25:337–379.
73. Crotty, S., M.M. McCausland, R.D. Aubert, E.J. Wherry, and R. Ahmed. 2006. Hypogammaglobulinemia and exacerbated CD8 T-cell-mediated immunopathology in SAP-deficient mice with chronic LCMV infection mimics human XLP disease. *Blood*. 108:3085–3093.
74. Chen, G., A.K. Tai, M. Lin, F. Chang, C. Terhorst, and B.T. Huber. 2005. Signaling lymphocyte activation molecule-associated protein is a negative regulator of the CD8 T cell response in mice. *J. Immunol.* 175:2212–2218.
75. Yin, L., U. Al-Alem, J. Liang, W.M. Tong, C. Li, M. Badiali, J.J. Medard, J. Sumegi, Z.Q. Wang, and G. Romeo. 2003. Mice deficient in the X-linked lymphoproliferative disease gene sap exhibit increased susceptibility to murine gammaherpesvirus-68 and hypo-gammaglobulinemia. *J. Med. Virol.* 71:446–455.
76. Moorman, N.J., D.O. Willer, and S.H. Speck. 2003. The gammaherpesvirus 68 latency-associated nuclear antigen homolog is critical for the establishment of splenic latency. *J. Virol.* 77:10295–10303.
77. Adler, H., M. Messerle, M. Wagner, and U.H. Koszinowski. 2000. Cloning and mutagenesis of the murine gammaherpesvirus 68 genome as an infectious bacterial artificial chromosome. *J. Virol.* 74:6964–6974.
78. Weck, K.E., M.L. Barkon, L.I. Yoo, S.H. Speck, and H.I. Virgin. 1996. Mature B cells are required for acute splenic infection, but not for establishment of latency, by murine gammaherpesvirus 68. *J. Virol.* 70:6775–6780.